ELSEVIER

Engineering Structures 23 (2001) 1383–1409

ENGINEERING STRUCTURES

www.elsevier.com/locate/engstruct

Experimental behaviour of end-plate beam-to-column composite joints under monotonical loading

L. Simões da Silva [a,*], Rui D. Simões [a], Paulo J.S. Cruz [b]

[a] *Departamento de Engenharia Civil, Universidade de Coimbra, Polo II, Pinhal de Marrocos, 3030-290 Coimbra, Portugal*
[b] *Departamento de Engenharia Civil, Universidade do Minho, Azurém, 4800 Guimarães, Portugal*

Received 19 July 2000; received in revised form 17 May 2001; accepted 18 May 2001

Abstract

An experimental research program on end-plate beam-to-column composite joints under monotonical loading is presented. The major focus relates to the identification of the contribution of the concrete confinement in composite columns to the behaviour of the joint, coupled with a thorough assessment of the various loading possibilities, ranging from symmetric and anti-symmetric loading on internal nodes to external nodes under hogging and sagging moments, typical in seismic regions. Comparison with current methodologies in the analysis of composite joints is also presented.

Keywords: Composite joints; Component method; Experimental; Strength; Stiffness; Ductility

1. Introduction

Composite construction has been increasingly used over recent decades (USA, Japan and some European countries) mostly in office buildings, commercial buildings, parking areas and bridges. However, despite the advantages it presents, composite construction is still scarcely used in some other countries, namely Portugal. The main reasons could possibly be the lack of experience, skilled workers and appropriate equipment on the one hand and on the other hand the nonexistence of codes for the design of these structures. The provisional version of Eurocode 4 presented design rules for the calculation and design of composite members (slabs, beams and columns), only including a few design principles for the design of joints between composite members. Recent research in this field resulted in a working document for the design of composite joints [1], and a specific section (Section 8) dealing with this subject in Draft 1 of the final version of Eurocode 4 [2].

In the past, steel joints were treated as pinned or rigid; nowadays, according to the new philosophy of design (Eurocode 3 (EC3) [3]) it has been stressed the need to take into account the real behaviour of the joint, usually falling between these two extreme cases and denoted as semi-rigid joints. As stated by recent studies [4,5], joints in composite structures, despite being usually stiffer than equivalent bare steel joints, still fall under the semi-rigid classification.

In the past, because of limited guidance in the design of composite joints, the contribution of the concrete part was usually neglected, design checks being carried out as for bare steel joints. Current design procedures, however, have proved the advantages [6] of taking into account the concrete, such as:

- weight reduction of beams and overall material;
- height reduction of beams and consequently, total height of buildings;
- better performance for service loads, with reduced cracking around the columns because of reinforcement in slabs.

The main parameters defining the mechanical behaviour of a joint are moment resistance ($M_{j,Rd}$), stiffness ($S_{j,ini}$ or S_j) and rotation capacity (ϕ_{Cd}). These parameters are obtained from the moment–rotation curve, typically represented in Fig. 1.

Characterising the behaviour of the joint through

* Corresponding author. Tel.: +351-239-797216; fax: +351-239-797217.
E-mail address: luis_silva@gipac.pt (L. Simões da Silva).

0141-0296/01/$ - see front matter
PII: S0141-0296(01)00054-2

Nomenclature

f_{ywb}	Yield strength of beam web
h_r	Distance from components at level r to the centre of the beam bottom flange
h_w	Height of beam web in compression
t_{fb}	Beam flange thickness
t_{wb}	Beam web thickness
z	Lever arm
z_{eq}	Equivalent lever arm
E	Young's modulus of steel
F_{bi}	Tensile forces at bolt row i
F_c	Compressive force at the lower flange of the beam
F_{cbw}	Compressive force in the beam web
F_{cp}	Compressive force at the contact surface between the column web and the concrete slab
F_i	Force developed in the component (spring) i
F_{tr}	Tensile force at the reinforcing steel
$K_{eff,r}$	Effective stiffness coefficient of an association of components in series at level r
K_{eq}	Equivalent stiffness coefficient of an association of components in parallel
K_i	Stiffness coefficient of the component (spring) i
$K_{i,r}$	Stiffness coefficient of a component at level r
L_i	Distance from the reinforcing steel to the centre of the beam bottom flange
L_r	Distance from the bolt row i to the centre of the beam bottom flange
M	Bending moment
$M_{j,Rd}$	Moment resistance of steel or composite joint
M_{Sd}	Applied bending moment
M_u	Ultimate moment of joint
P	Vertical force
S_j	Secant stiffness of steel or composite joint
$S_{j,ini}$	Initial stiffness of steel or composite joint
Δ_i	Deformation of the component (spring) i
ϕ	Joint rotation
ϕ_{Cd}	Joint rotation capacity
ϕ_M	Joint rotation corresponding to elements of connection
ϕ_{max}	Maximum rotation observed during testing
ϕ_{Total}	Total joint rotation
ϕ_u	Joint ultimate rotation
ϕ_V	Joint rotation corresponding to distortion of column web panel

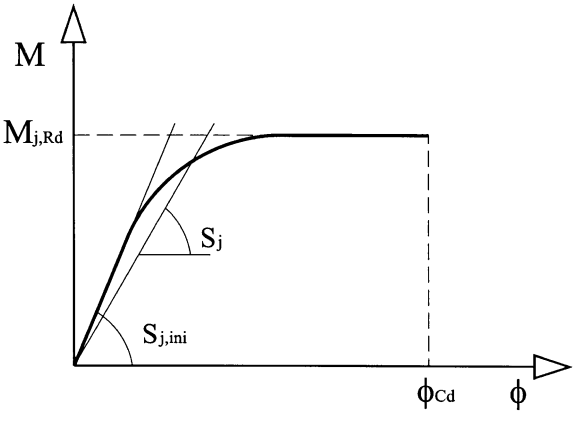

Fig. 1. Typical moment–rotation curve of a joint.

moment–rotation curves, the bending moment is evaluated in the contact section between the column flange and the beam end plate. The rotation of the joint is described as the variation of the angle between the tangent to the beam axis and the tangent to the column axis, after deformation (Fig. 2). In general, the rotation of a joint has two components: (i) Rotation due to the deformation of the components situated in the connection zone — connection rotation ϕ_M (Fig. 2(a)) and (ii) Rotation due to the horizontal column web deformation due to the shear force — shear panel rotation ϕ_V (Fig. 2(b)).

In accordance with EC3 and EC4, joints are classified in terms of stiffness (rigid joints, semi-rigid and pinned) and moment resistance (full strength and partial strength). The classification of a joint depends on its

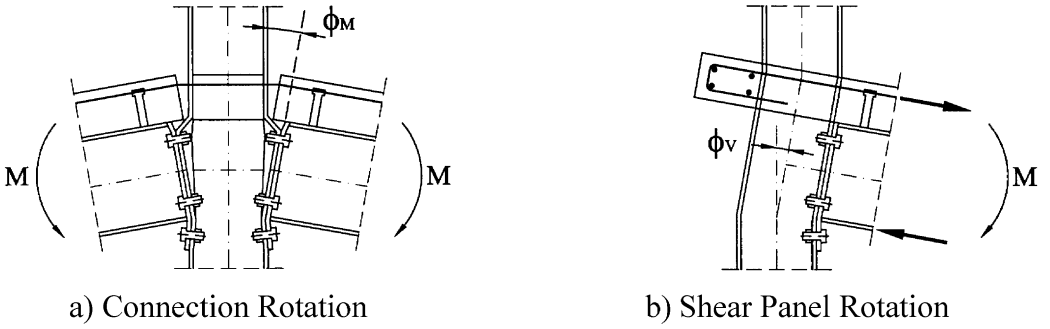

Fig. 2. Joint rotation.

properties (moment resistance and stiffness) and its influence on the global structural behaviour.

A review of research in this field shows that in the past few years knowledge of the behaviour of beam-to-column composite joints has advanced extraordinarily. Experimental research on composite joints started in the seventies. Zandonini [4] reviewed the major experimental research projects prior to 1989. In his paper, tests performed by Johnson and Hope-Gill, Owens and Echeta, Van Dalen and Godoy, Johnson and Law, Benussi et al. and Ammerman and Leon are described, which are summarized here in Table 1.

From 1990 to present, tests performed by Davison et al. [7], Leon [8], Puhali et al. [9], Altmann et al. [10], Aribert and Lachal [11], Xiao et al. [12], Anderson and Najafi [13], Bode and Kronenberger [14], Li et al. [15] are summarized in Table 2.

In addition, the static behaviour of composite joints inserted in full-scale frames was investigated in the universities of Nottingham, Trento and Trieste [16–19]; in this research program, two series of 2-storey 3D frames were tested, using the same joints previously tested in isolation [15].

Based on the works of Zandonini [4] and Choo [20] and on the results of the experiments described above and similar results from the tests held by Bernuzzi et al. [21], Tschemmernegg [22], Badran [23], Ren [24], Shanmugam [25] and Wong et al. [26] it can be concluded that:

- The reinforced concrete slab, with a certain amount of continuity reinforcing steel, linked to the beam by means of connectors, has a very significant effect in the mechanical properties of a composite joint. The lighter the steel joint, the bigger the effect [24]. Fairly stiff joints can be achieved using quite simple steel joints, reaching hogging moments of the same order of magnitude as the composite section [7–10,25].
- Resistance and stiffness increase with increasing slab reinforcement [12,13]. This tendency, however, only exists up to a certain limiting value; for higher percentages of reinforcement, components in the shear or

Table 1
Tests in composite joints previous to 1989

Authors (date)	No. of tests	Description	Main parameters investigated
Johnson and Hope-Gill (1972)	5	Symmetric connections in internal nodes; bottom flange cleat connection; composite beam and steel column.	Beam web slenderness; ratio between the force in the reinforcing steel and in the profile.
Owens and Echeta (1981/82)	5	Symmetric and asymmetric connections (external nodes); cleat and flush end plate connections; composite beam and steel column.	Behaviour of external nodes and internal nodes; different steel connections; different ratios moment/shear force.
Van Dalen and Godoy (1982)	4	Symmetric connections in internal nodes; cleat joint; composite beam and steel column.	Displacement between the steel beam and the concrete slab; different ratios of reinforcing steel.
Johnson and Law (1983)	6	Symmetric joints in internal nodes; flush end plate steel joint; composite beam and column.	Shear connectors; column confinement effect; moment in both the strong and weak column axes; ratio between the slab thickness and the steel beam depth; effect of the axial force in the column.
Benussi et al. (1986/87)	4	Symmetric joints in internal nodes with slightly asymmetrical loading; flush or extended end plate; composite beam and steel column.	Interaction slab–column; effect of high ratios of reinforcing steel in the compression zone stability.
Ammerman and Leon (1986/87)	2	Symmetric joints in internal nodes; cleat joint; composite beam and steel column.	Cleat joints; basis of comparison for cyclic tests.

Table 2
Tests in composite joints performed between 1990 and the present

Authors (date)	No of tests	Description	Main parameters investigated
Davison et al. (1990)	19	7 steel joints and 12 composite joints, with bottom flange cleat and web cleat.	Direction of the sheet metal decking; column orientation (weak and strong axis joint); internal nodes and external nodes; different amounts and arrangement of reinforcement steel in the slab.
Leon (1990)	6	Composite joints with bolted cleats.	Behaviour of internal nodes under static monotonic symmetrical loading (zero moment in column)
Puhali et al. (1990)	6	Internal nodes under symmetric load conditions.	Flexibility of the steel joint beam–concrete slab; interaction between the slab and the column; asymmetric load sequences (different left and right moments).
Altmann et al. (1991)	56	Internal and external nodes.	Ratio of stiffness between beam and column; number and thickness of cleats; percentage of reinforcement.
Aribert and Lachal (1992)	10	Internal nodes, under symmetric load conditions.	Beam and column sections depths; flush or extended end plate; shear connectors and the degree of interaction between the steel beam and the concrete slab.
Xiao et al. (1994)	20	Internal and external nodes, under monotonic load conditions.	Evaluation of the resistance, stiffness and rotation capacity, for different steel joints and different amounts of reinforcing steel.
Anderson and Najafi (1994)	6	Internal frame nodes, undersymmetric and monotonic load conditions.	Percentage of reinforcement; depth of steel beam and type of end-plate (flush or extended).
Bode and Kronenberger (1994)	15	Internal nodes joints under symmetric load.	Influence of the steel beam and the concrete slab.
Li et al. (1994)	7	Internal nodes beam-to-column joints.	Different right and left bending moments and different ratios between the shear force and the bending moment.

compression zone control the behaviour of the joint. Consequently, in a composite joint subjected to negative moment, the higher the longitudinal slab reinforcement, the greatest the care in designing the compression or shear zones, stiffeners being often required [12].

- The rotation capacity, despite being smaller when compared to the bare steel joint, is normally sufficient (bigger than 25 mrad according to Aribert [11]) in order to allow the redistribution of bending moments and the plastic analysis of the structure. Ductility normally increases with increasing reinforcement, being normally quite reduced whenever standard mesh reinforcement for load distribution is used in slabs [7,12,13].
- The degree of interaction between the steel beam and the concrete slab greatly affects the joint response [11,14,23].
- The type of steel joint has a great influence on the behaviour of the composite joint. Different results were obtained from tests carried out on composite joints in which the steel joint consisted of flush or extended end plates or cleats [10,12].
- The interaction between the slab and the column has a significant influence under asymmetric load conditions and whenever the resistance of the reinforcement is higher than the web shear resistance of the column, or the compression resistance in the contact surface between the slab and the column flange [15,19].
- Anchorage of reinforcement in external nodes highly affects the behaviour of the joint. Some authors believe that these joints should be considered as pinned, unless effective anchorage of the reinforcement is provided [7,12]. According to Elnashai [27], effective anchorage is achieved whenever at least 40% of the longitudinal reinforcement circumscribes the column.
- The use of columns embedded in concrete has a significant effect in the behaviour of the joints, the concrete covering the web of the column contributing to the behaviour of the column, similarly to stiffeners [25].
- In the case of slabs with metal decking, the direction of the corrugations influences the behaviour of the joint. If the corrugations are parallel to the beam, the area of concrete is bigger and the metal decking effectively contributes towards the resistance of the joint [12].
- The relation shear force/bending moment only sig-

nificantly influences the resistance of the joint when the value of the shear force is high compared to the web shear resistance of the beam [12,15].
- Tests results for joints inserted in frames revealed a decrease in strength and stiffness of the same joints when tested in isolation [17–19]; this decrease was basically the result of additional internal forces not present in isolated tests. Additionaly, those tests proved that joint ductility was sufficient for full plastic hinges to form in the beams, thus opening the way to the use of plastic methods of analysis of composite frames [16,17].

In spite of this extensive experimental work and the resulting analytical and numerical models that, under certain conditions of geometry and load, are able to yield good results, other types of nodes, such as external nodes, nodes with joints in several directions, among others, are not so well covered in the literature. Also, though symmetric loading conditions (equal-bending moments from one and the other side of the column) represent quite a common situation, there are some other situations in which the stresses (specially the bending moments) from one side of the column to the other are completely different, as is the case of unequal beam lengths or different loads or frames subjected to horizontal loads (for instance the seismic action), where the moments can even have opposite signs from one side of the column to the other. Finally, most joints studied in the past corresponded to joints between composite beams and steel columns, while joints with composite columns may be quite advantageous.

Thus, it is the objective of this paper to present a series of experimental test results which will be used to widen and validate current methodologies for the analysis of steel and composite joints. More specifically, special attention will be given to the effect of column confinement on the behaviour of the joint.

2. Experimental test program

2.1. Introduction

A detailed description of an experimental testing program in composite beam-to-column joints, performed at the Civil Engineering Department of the University of Coimbra, is presented in this section. The test program includes 8 prototypes, being 4 in internal nodes and 4 in external nodes. The description of each model includes the geometric definition, the material properties and the testing and instrumentation procedures.

The prototypes were defined such that they could reproduce the joints in a common framed structure, with spans of about 7 m, 4 m spacing between frames, live loads up to 4 kN/m^2 and a high energy dissipation capacity and a good fire resistance. According to the objectives of this study, the steel joint is the same in all prototypes, corresponding to a very common joint in which the beam is connected to the column by one end plate, welded to the beam and bolted to the column. The prototypes cover internal and external nodes and were defined such that they could reproduce the local behaviour of the real framed structure, with the identification of the points of zero moment for the columns, physically built as pinned joints, and the application of loading in the beams at the cross-sections where curvature changes (points of inflexion) [28] (Fig. 3).

The choice of geometry and materials (steel sections, bolts, concrete and steel resistances, etc.) was done in accordance with Eurocodes 2, 3 and 4, taking into account the laboratory restrictions in terms of the size of the loading frame and the hydraulic jacks. A brief description of the tests is presented in Table 3 where $M+$ and $M-$ denote positive and negative bending moments, respectively, corresponding to upward or downward load application.

2.2. Prototype description

As described in Table 3, four tests were performed in internal nodes, tests E1 and E2 corresponding to the prototype arrangement between composite beams and a steel column shown in Fig. 4 and tests E7 and E8 between composite beams and a composite column, illustrated in Fig. 5.

As for the internal nodes, four tests were performed in external nodes, tests E3 and E4 corresponding to a steel column and described in Fig. 6, and tests E5 and E6 corresponding to a composite column and illustrated in Fig. 7.

In all cases, the beams consist of an IPE 270, rigidly connected to a reinforced concrete slab (full interaction) by 8 block shear connectors. The slab, 900 mm wide (was established in accordance with EC4) and 120 mm thick, is reinforced with 10∅12 longitudinal bars (1.05% of the total concrete area) and 10∅8 transversal bars per meter (corresponding to the minimum reinforcement imposed by EC4 for control of cracking), with 20 mm cover. In the external node prototypes, the two rebars closer to the beam axis go round the column, while the remaining rebars are anchored as shown in Fig. 6 and Fig. 7. The steel joint consists of a 12 mm thick end plate, welded to the beam and bolted to the column flange through 6 M20 bolts (class 8.8), tightened with a torque of 150 Nm. The end-plate is flushed at the top and extended at the bottom, in order to achieve similar behaviour under positive and negative moments.

The steel column is the same in all the tests (HEA 220), being embedded by concrete (300×300 mm) in tests E5, E6, E7 and E8, with longitudinal reinforcement of 4∅12, with one bar in each corner of the section and

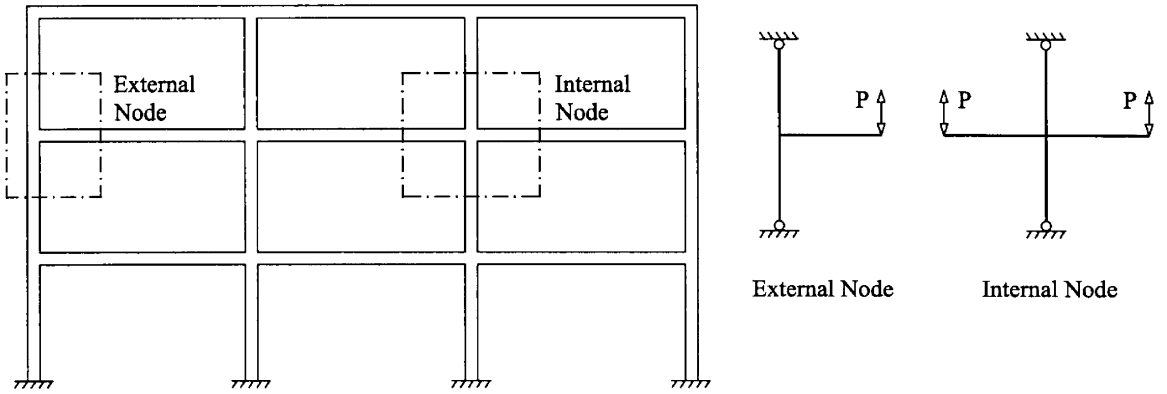

Fig. 3. Nodal configurations.

Table 3
Prototype definition

Test	Joint location	Column section	Load type (left/right moments)
E1	Internal Node	Steel	($M-/M-$)
E2	Internal Node	Steel	($M+/M-$)
E3	External Node	Steel	($M-$)
E4	External Node	Steel	($M+$)
E5	External Node	Composite	($M-$)
E6	External Node	Composite	($M+$)
E7	Internal Node	Composite	($M-/M-$)
E8	Internal Node	Composite	($M+/M-$)

stirrups consisting of ∅6 bars 0.08 m apart. The following materials were chosen: S235 in the steel components, steel class 8.8 in the bolts, steel A400 NR in the reinforcing bars; the concrete, with a composition optimised using Faury's method [29] and consisting of Standard Cement Portland=400 kg, cleaned sand of river Tejo=648 kg, gravel 8/12=438 kg, gravel 12/25=780 kg and water=192 litres, can be classified as a C35/45. The concrete composition was corrected for the various tests according to the humidity of the aggregates.

The loads were applied to the beams 1.40 m from the column face with two hydraulic actuators with a capacity of 200 kN and 600 kN, and maximum displacement of 200 mm and 100 mm, respectively. The need to apply the loads both downward and upward required a special setup, later descibed in Section 2.3. In tests E1 and E7, loading is symmetric (both loads downward) while in tests E2 and E8 loading is asymmetric (one load upward and the other downward).

In tests E3 and E5 the load is applied downward, while in tests E4 and E6 it acts upward.

2.3. Laboratory equipment and instrumentation

The prototypes were mounted in a reaction frame of the Structures and Materials Laboratory shown in Fig. 8 together with the required accessories used in these tests. The beams and the columns of the reaction frame are HEB 300. As described before, loading was applied using two hydraulic jacks anchored in a mid point to maintain the verticality during the tests. Application of loading both upward and downward required a special setup composed of a group of plates in the top and bottom faces, connected by four M20 bolts, with a length of 80 cm, also enabling the inclusion of the load cells.

To support the prototypes and to ease dismounting operations, a base rigidly connected to the concrete reaction slab is used, which enables the free rotation of the column base. At the top of the column, a rigid simple support was added, connected to the top beam of the reaction frame, also allowing the introduction of the load cells. At the ends of the beams vertical guides were placed to restrain lateral displacements.

The instrumentation was planned in order to enable the evaluation of the main mechanical properties: strength, stiffness and rotation capacity. Those properties are essentially obtained through the moment–rotation relationship of the joint. Having in mind the component method, isolating the contribution of each component to the global behaviour of the joints was attempted by placing the various measuring devices appropriately.

The instrumentation used included displacement transducers, extensometers, load cells and inclinometers. A TDS601-TML datalogger was used to collect all the

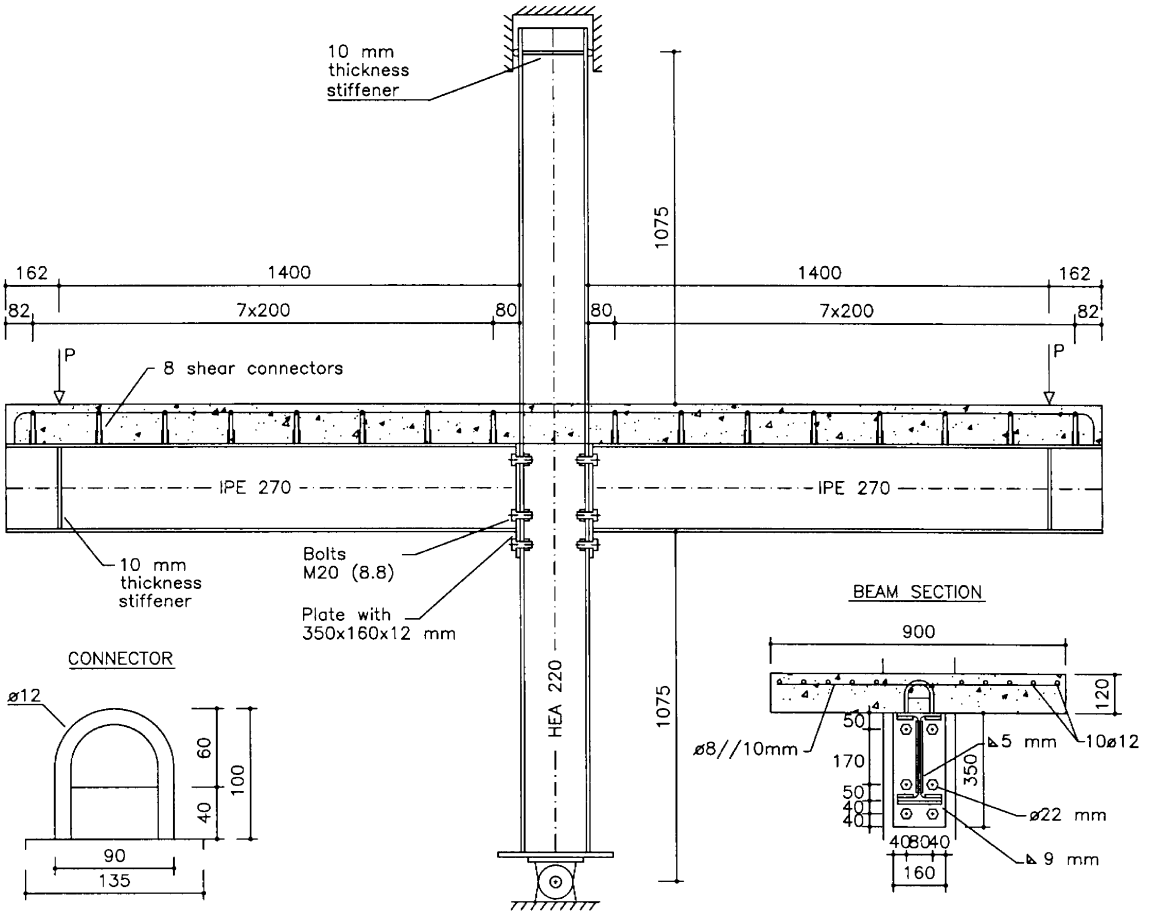

Fig. 4. Internal node, bare steel column.

measured values. Figure 9 represents the instrumentation used in one prototype. Figure 10 illustrates the instrumentation of one model. Figures 11 to 13 describe in detail the use of the various measuring devices for the different joint components, the same notation being used as in Fig. 9.

- The load cells placed at the points of application of the vertical loads (1.40 m from the face of the column) and upper support enabled the evaluation of all the forces acting on the joint throughout the test;
- Displacement transducers were used with multiple purposes:
  - Evaluation of rotation, by subtracting the readings between two paralell transducers;
  - Evaluation of vertical displacement along the beams;
- Unidirectional strain gauges placed on beam flanges and web, column web and flanges, longitudinal and transversal slab reinforcement, longitudinal and transverse composite column and concrete surface (Fig. 11 and 13) enabled the evaluation of stresses in the main components of the joint. Special protection techniques were used to place the strain gauges in the reinforcement and column flanges and web envolved in concrete. Special strain gauges were used for the bolts, placed inside a drilled hole of diameter 2 mm, as shown in Fig. 12;
- Multi-directional strain gauges (rosettes) completely characterised the stress-state in the column and beam webs around the joint.

3. Mechanical properties of materials

The actual properties of the materials were established for the various components, beam and columns steel sections (web and flanges), steel plates, bolts, reinforcing steel and concrete, according to the applicable standards [3,31–33] for steel specimens in a universal testing machine and the relevant standards [34,35] for concrete specimens.

Table 4 describes the results of the tests performed in the steel components. The presented values correspond to the average of three tested specimens. Some steel components (beams, columns, end plates and bolts) where bought in two different stages. In Table 4 both

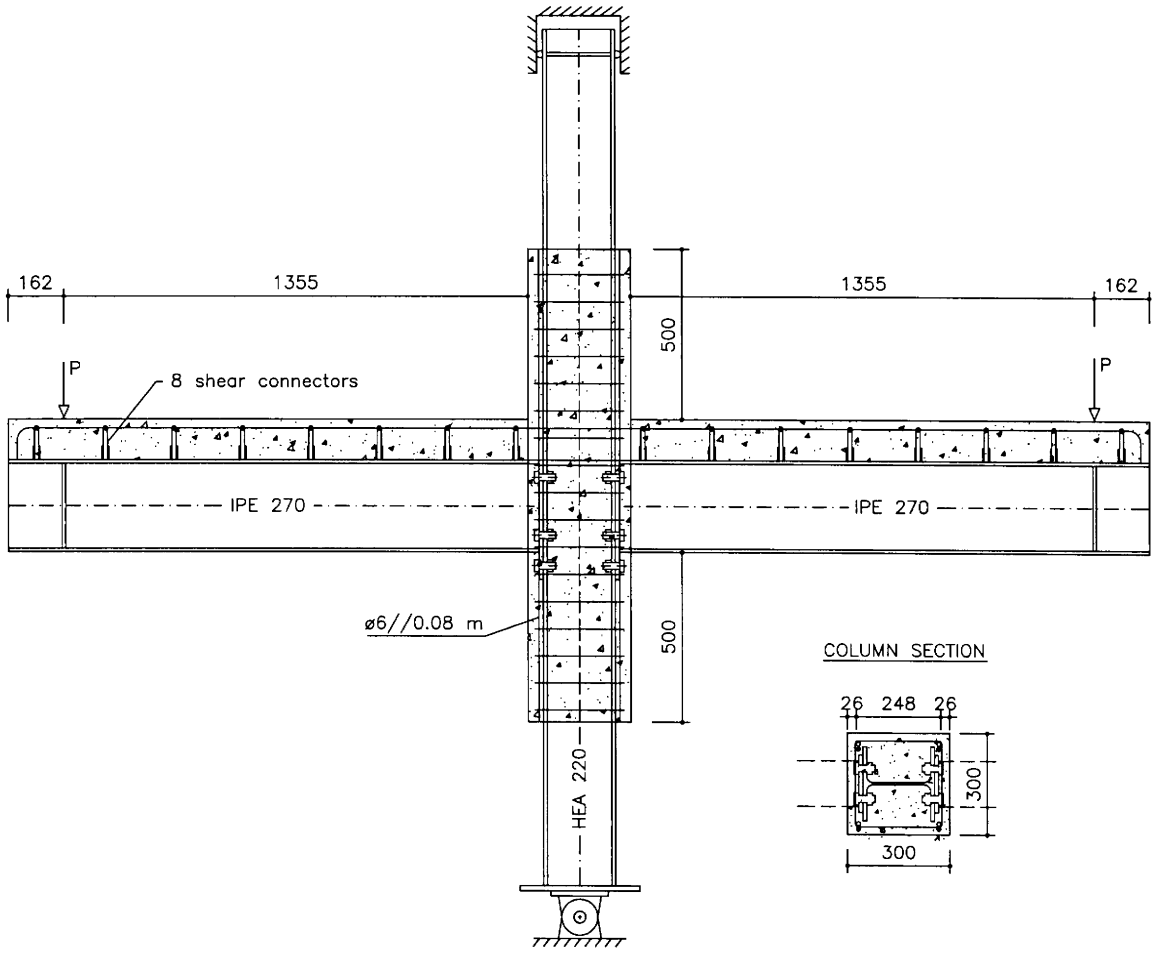

Fig. 5. Internal node, composite column.

lots are presented. Lot 1 was used in the tests E1 to E4 and lot 2 was used in tests E5 to E8.

As can be observed in Table 4, the steel supplied for the columns in the second lot has considerably more strength than the other steel elements.

Table 5 summarises the results of the tests performed in the concrete specimens. The presented values correspond to the average of three tested specimens.

The real dimensions of the elements were measured. The nominal dimensions and the average of the real dimensions are presented in Table 6. In the evaluation of the thicknesses an ultra-sound equipment was used. Table 7 presents the average of the real thicknesses.

4. Results and discussion

4.1. Test execution

The monotonic static tests were performed under force control in the elastic phase and displacement control in the plastic phase.

The comparative analysis of the results of the tests with steel and composite columns is crucial for the evaluation of the effect of concrete confinement. However, this goal was not completely achieved due to the higher strength of the steel used in the composite columns (tests E5 to E8 and steel lot 2). In fact, the increase in the strength of the joints of tests E5 to E8 is not only due to the enveloping concrete, but also results from the higher yield strength of the steel. Consequently, to allow direct comparison between bare steel and composite column tests, an analytical correction in the experimental moment–rotation curves of the joints with composite columns (tests E5 to E8) was introduced by replacing the actual yield strength of steel for these joints by the yield strength from the corresponding bare steel column tests (tests E1 to E4). This analytical correction was implemented using the methodology presented in Simões [36], based on Annex J of EC3 and Section 8 of EC4 and briefly described later. These corrected experimental test results are henceforth denoted as E5* to E8*.

As described before, strains were measured for all the main components. Despite the importance of these results, this amount of information cannot be presented

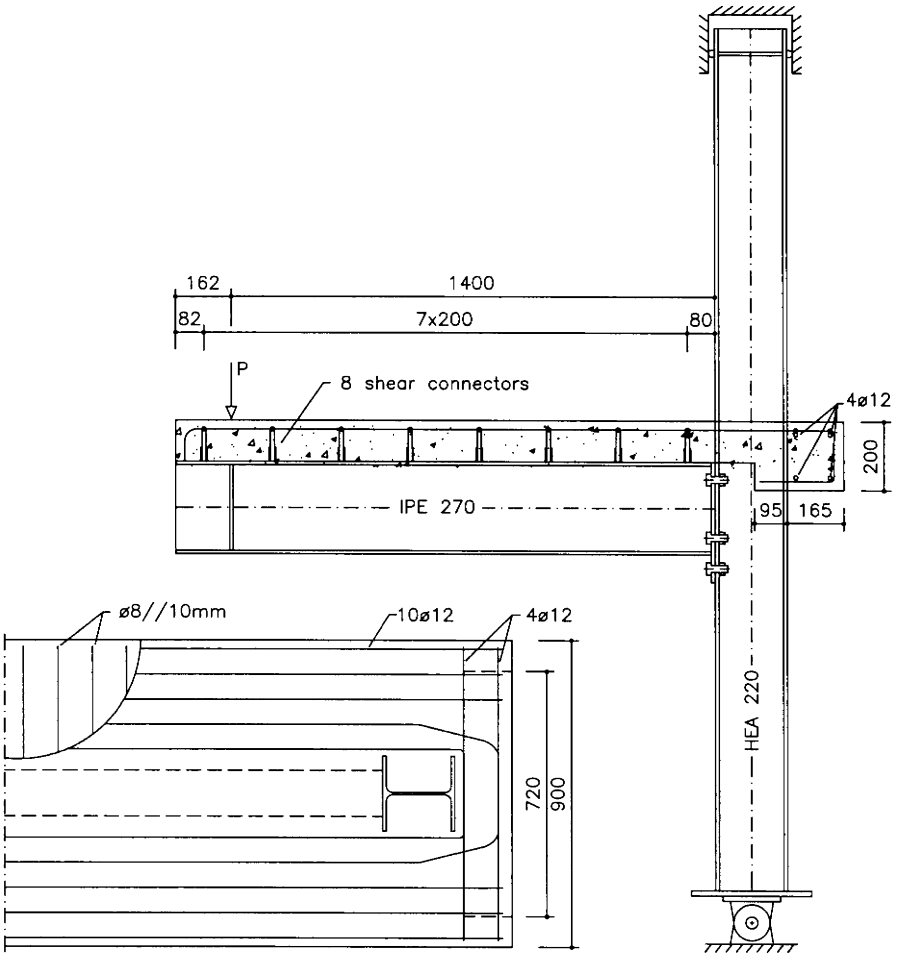

Fig. 6. External node, steel column.

in this paper, all results being available in [36]. Because the bending moment–stress curves are obtained using Hooke's law, their validity is limited by the yield stress of the corresponding steel; in the following, and for the moment–stress diagrams only, solid lines refer to steel from the first lot (tests E1 to E4), while broken lines correspond to the second lot (tests E5 to E8).

4.2. Tests in internal nodes

4.2.1. Description of test results

Figures 14 to 16 show the moment–rotation curves in the internal node tests. The moment–rotation curves of Fig. 14 take into account only the deformation of the connection, ϕ_M. For tests E1 and E7, those curves coincide with the total joint rotation (ϕ_{Total}), because of symmetry of loading. Figures 15 and 16 present the total moment–rotation curves (ϕ_{Total}) and the contribution of the column web deformation in shear (ϕ_V).

Figure 17 compares the results of the tests E1 and E2 (steel column) with the analytical results E7* and E8* obtained from tests E7 and E8 (composite column) introducing the previously described correction in the steel strength of the columns.

4.2.2. Discussion and evaluation of test results

Collapse of test E1 was mostly caused by column web local buckling at the bottom level of the beam, due to the development of high compressive forces (Fig. 18). Additional contributions to the joint deformation were the bending of the column flange and the end-plate (T-Stub) and the yielding of the longitudinal reinforcing steel closer to the column (Fig. 19). Figure 21 shows the joint elements and the slab after testing.

In the test E7, the embedding concrete in the column changed the failure mode as the column web remained elastic (Fig. 18). Failure was due to yielding of the longitudinal slab reinforcement (Fig. 19) and yielding of the bottom beam flange and web (Fig. 20). The top bolt rows also presented very high strain levels. Figure 22 illustrates the crack pattern in the slab after failure.

The behaviour of joints such as occurred in test E1 is not desirable. Effectively, failure was brittle since it was due to buckling of the column web for a rotation of only

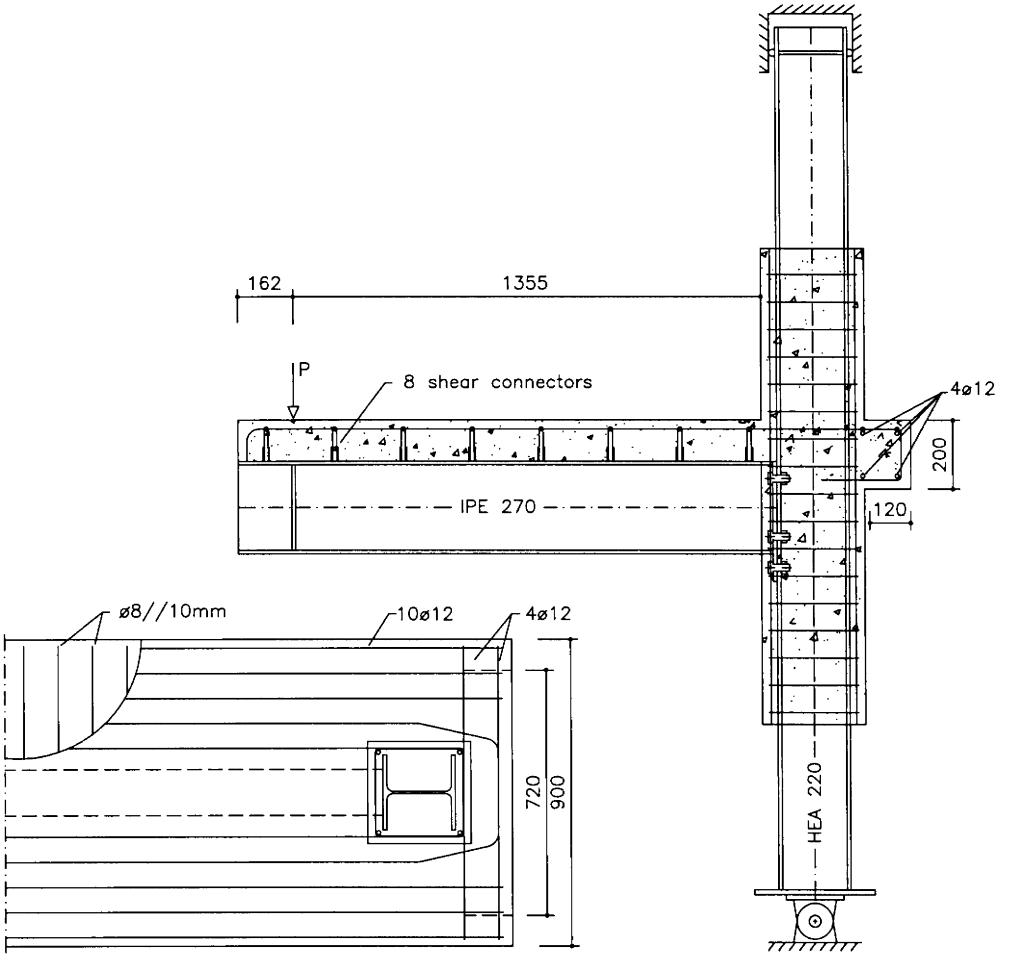

Fig. 7. External node, composite column.

7.6 mrad. The concrete confinement of the column introduced in test E7 had a beneficial effect, increasing strength and stiffness, without a significant reduction of the rotation capacity. In this test, the weak components were outside the composite column zone, as it is convenient for a structure under seismic actions.

For test E2, first test with anti-symmetric loading, failure is almost exclusively due to the horizontal shear of the column web (panel zone). Figure 23 shows this test after failure.

Despite the concrete embedding of the column in test E8, failure still occurs because of horizontal shear of the column web (panel zone). Additionally, yielding of the longitudinal reinforcement closer to the column (Fig. 19), yielding of the bottom beam flange in the negative moment side and crushing of the slab concrete in the positive moment side also contribute to the observed failure. Figure 24 shows the crack pattern in the column and the global deformation of the joint after testing.

Test E2 presented a high rotation capacity (around 45 mrad) accompanied by low moment resistance. The composite column used in test E8 had a beneficial effect since strength and stiffness increased despite the reduction of rotation capacity (still reaching around 30 mrad). In both cases, however, the weak components were still inside the column.

Table 8 summarises the mechanical properties of joints E1, E2, E7 and E8, as well as the identification of the main failure mode for these tests.

In all cases the joints are classified as partial strength and semi-rigid (according to Eurocode 3 Annex J, and with the assumed sway frame with 7 m long beams).

4.3. Tests in external nodes

4.3.1. Description of test results

Figures 25 to 27 show the moment–rotation curves in the external node tests. Figure 25 represents the moment–rotation curves corresponding solely to the connection deformation (ϕ_M), while Figs 26 and 27 present the total moment–rotation curves (ϕ_{Total}) and the contribution of the column web in shear (ϕ_V). Figure 28 compares the results of the tests E3 and E4 (steel column) with the analytical results E5* and E6* obtained from tests E5 and E6 (composite column) again introducing

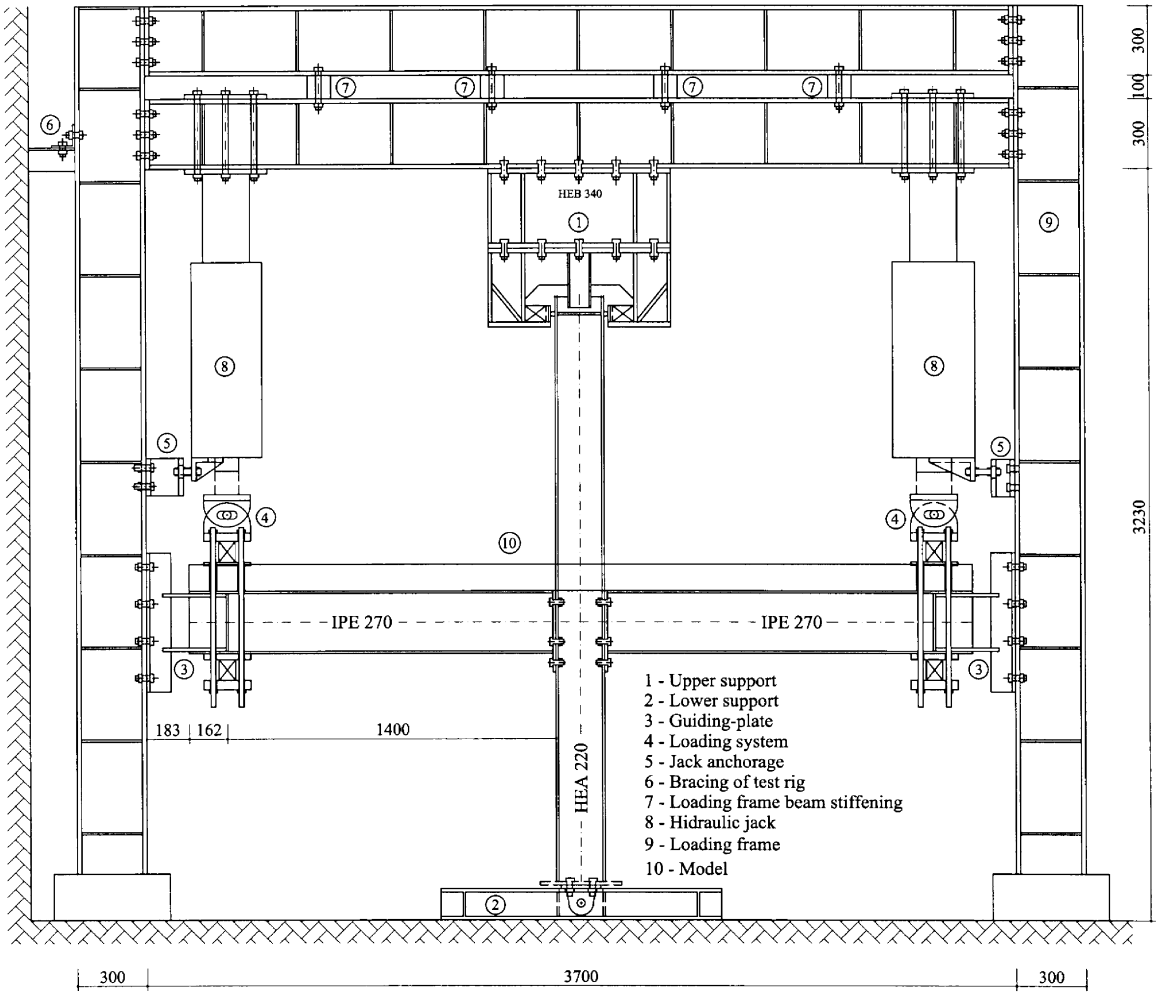

Fig. 8. Test rig.

the previously described correction in the steel strength of the columns.

4.3.2. Discussion and evaluation of tests results

In external node tests, due to the asymmetrical loading, the horizontal shear deformation of the column web (panel zone) is the main failure mode, unless if this zone is conveniently stiffened. Effectively, this was the failure mode of test E3 and E4 (Figs 26 and 29).

In test E3 the yielding of the longitudinal reinforcing steel closer to the column and the cracking of the concrete slab in the anchorage zone constituted a second contribution. In test E4 the compression in the concrete slab near the column was very high, causing the concrete to crush and contributing to failure.

In test E5, failure was due to yielding of the slab longitudinal reinforcement and yielding of the bottom beam flange and web, the top bolt row almost reaching failure.

In test E6 failure was mainly due to bending of the column flange and end-plate, together with yielding of the tension bolts (second and third rows). Figures 30 to 33 show tests E3 to E6 after failure.

Table 9 summarises the mechanical properties of joints E3, E4, E5 and E6, as well as the identification of the main failure mode for these tests.

Based on the results of these experimental tests, and under static monotonic loads, the anchorage arrangement adopted for the longitudinal slab reinforcement performed adequately, failure never occurred because of insufficient anchorage.

The joints between the composite beams and the steel columns had a very ductile behaviour, the main failure reason being the horizontal shear force in the column web. Moment resistance was bigger than that obtained disregarding the slab contribution, as recommended by some researchers [37].

The global behaviour of the external node joints was significatively improved by the addition of the concrete in the composite columns (tests E5 and E6). In those

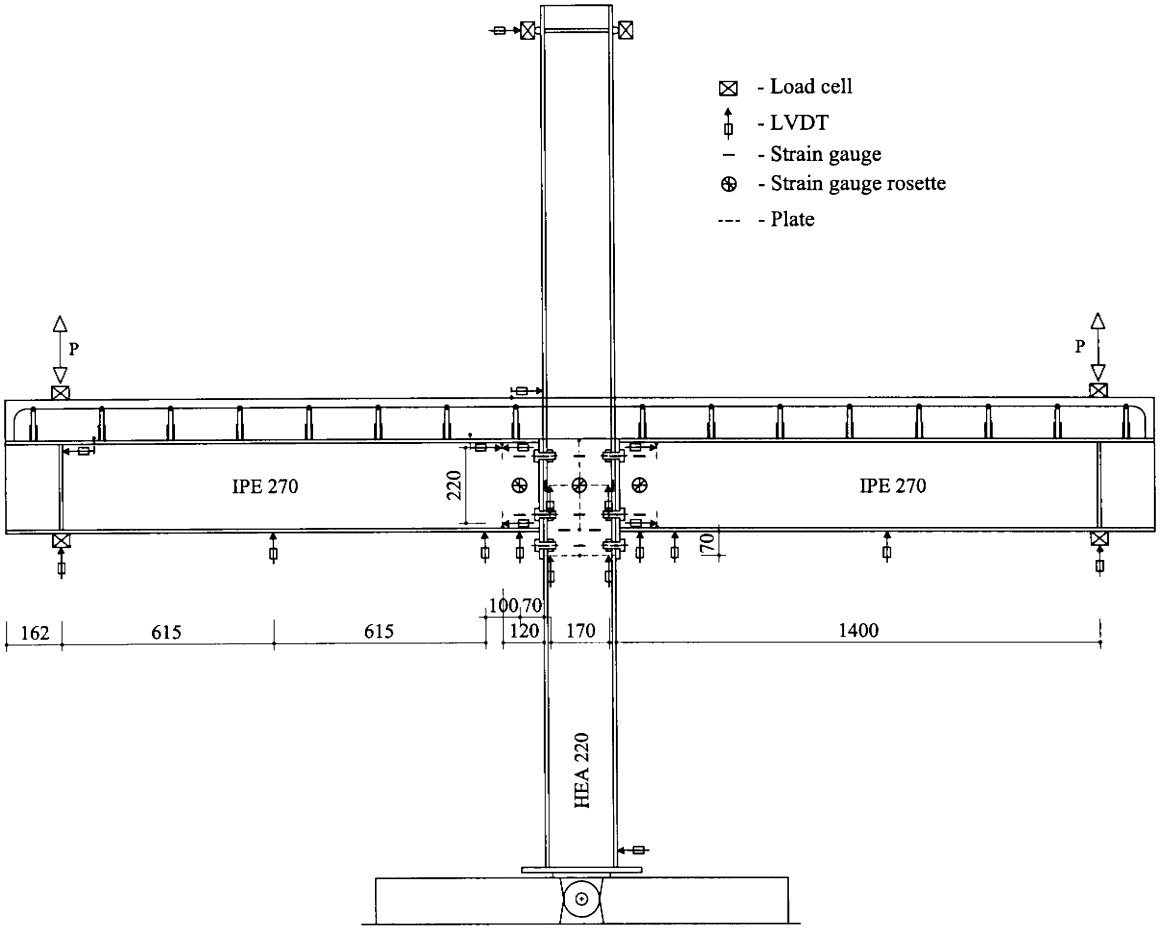

Fig. 9. Instrumentation of the prototypes (internal node).

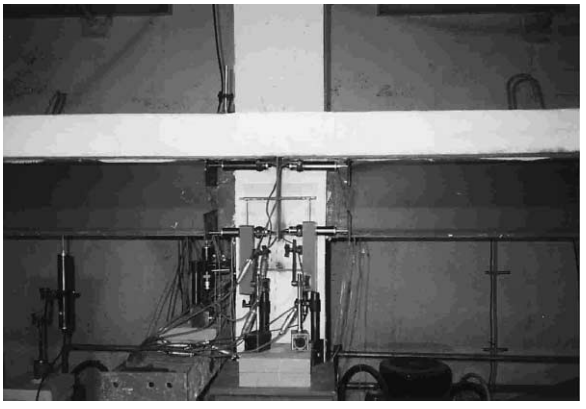

Fig. 10. Instrumentation of prototypes.

tests, the weak zone was displaced from the panel zone with an important increase in the resistance and stiffness, without a significant reduction in ductility.

In all cases the joints can be classified as partial strength and semi-rigid (according to Eurocode 3 Annex J, and with the assumed sway frame with 7 m long beams).

5. Analytical evaluation

Adopting as a starting point the research results produced by various authors over the past few years which formed the basis of Eurocodes 3 and 4 and companion documents [1,30,38,39], an analytical methodology to evaluation of the behaviour of end-plate beam–column composite joints under monotonical loading was developed by the authors [36], briefly described below.

The analytical behaviour of a beam–column composite joint (moment–rotation curve) is based on the component method (adopted in EC3 and EC4), whereby each component is idealised as a spring characterised by a non-linear force–deformation curve. The method can be subdivided into three stages:

(i) Identification of the fundamental components in the tension, compression and shear zones of the joint;
(ii) Evaluation of the resistance, the stiffness and the deformation capacity of each component;
(iii) Assembly of the different components in order to evaluate the global behaviour of the joint.

Considering an internal node subjected to hogging

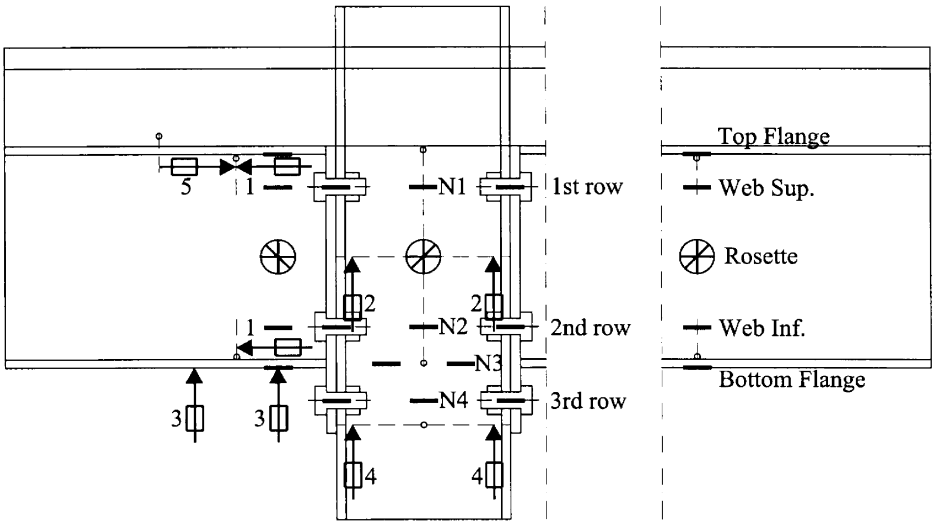

Fig. 11. Detail of the instrumentation of the nodal zone.

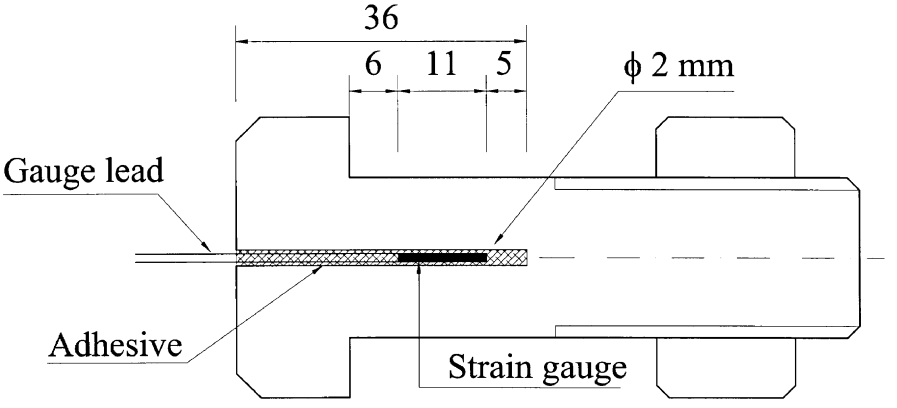

Fig. 12. Detail of the instrumentation of a bolt.

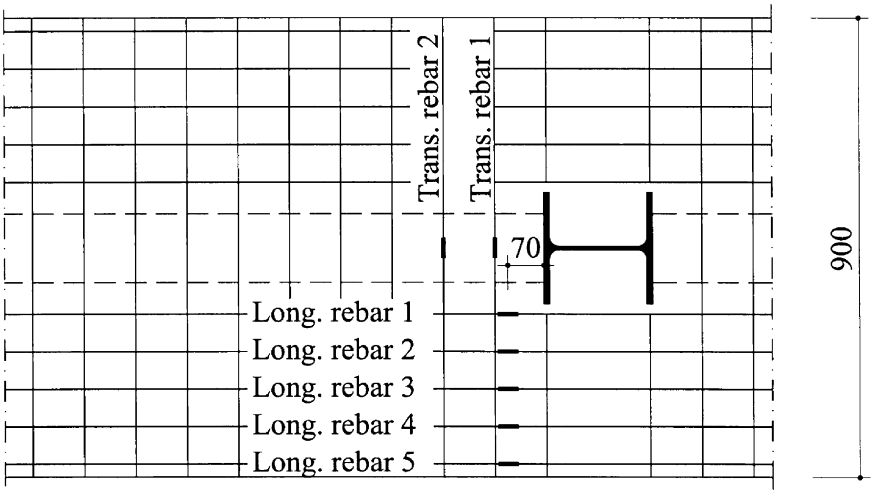

Fig. 13. Detail of the instrumentation of the slab reinforcement.

Table 4
Mechanical properties of steel components

	Element		Yield strength (MPa)	Ultimate strength (MPa)	Yield strain (%)	Ultimate strain (%)	Modulus of elasticity (MPa)
Lot 1	Beam	Web	306	439	23.9	31.8	198
	(IPE270)	Flange	267	415	24.4	36.1	203
	Column	Web	328	476	22.1	31.5	198
	(HEA220)	Flange	303	459	20.6	34.5	211
	End-plate		283	437	23.7	31.0	206
	Bolts		–	939	–	–	219
Lot 2	Beam	Web	345	508	21.3	31.8	203
	(IPE270)	Flange	311	493	20.9	34.9	208
	Column	Web	495	589	17.5	25.6	204
	(HEA220)	Flange	479	578	13.9	21.2	213
	End-plate		304	460	23.7	36.6	217
	Bolts		–	1008	–	–	209
Connectors			376	645	17.1	33.3	175
Rebar ∅12 mm			541	639	15.0	25.6	205
Rebar ∅8 mm			513	600	16.4	23.2	212
Rebar ∅6 mm			470	614	13.6	17.6	208

Table 5
Mechanical properties of concrete cylinder specimens

Test (age of concrete)	Unit weight	Compression strength (MPa)	Modulus of elasticity (GPa)
E1 (23 days)	2.32	27.65	31.3
E2 (16 days)	2.36	29.98	31.9
E3 (16 days)	2.37	39.00	34.3
E4 (15 days)	2.35	34.51	33.2
E5 (16 days)	2.37	28.90	31.6
E6 (15 days)	2.31	27.76	31.3
E7 (34 days)	2.35	29.57	31.8
E8 (15 days)	2.33	32.31	32.6

Table 6
Nominal dimensions and average of the real dimensions (mm)

	Column (HEA 220)		Left beam (IPE 270)		Right beam (IPE 270)		Left end-plate		Right end-plate	
	Height	Width	Height	Width	Height	Width	Height	Width	Height	Width
Nominal	210	220	270	135	270	135	350	160	350	160
LOT 1 (E1 to E4)	208.5	219.8	270.8	136.0	270.5	135.5	350.0	160.0	350.0	160.0
LOT 2 (E5 to E8)	212.2	222.5	270.0	135.8	270.2	135.9	348.4	160.3	348.6	160.3

Table 7
Average of the real thicknesses (mm)

	Column (HEA 220)			Left beam (IPE 270)			Right beam (IPE 270)			End-plate	
	Web	Flanges		Web	Flanges		Web	Flanges		Left	Right
		Top	Bottom		Top	Bottom		Top	Bottom		
Nominal	7.0	11.0	11.0	6.6	10.2	10.2	6.6	10.2	10.2	12.0	12.0
LOT 1 (E1 to E4)	7.1	10.4	10.5	6.8	9.8	9.8	6.8	9.7	9.7	12.0	11.9
LOT 2 (E5 to E8)	7.2	10.5	10.6	6.9	9.9	10.0	6.9	9.9	10.1	12.4	12.4

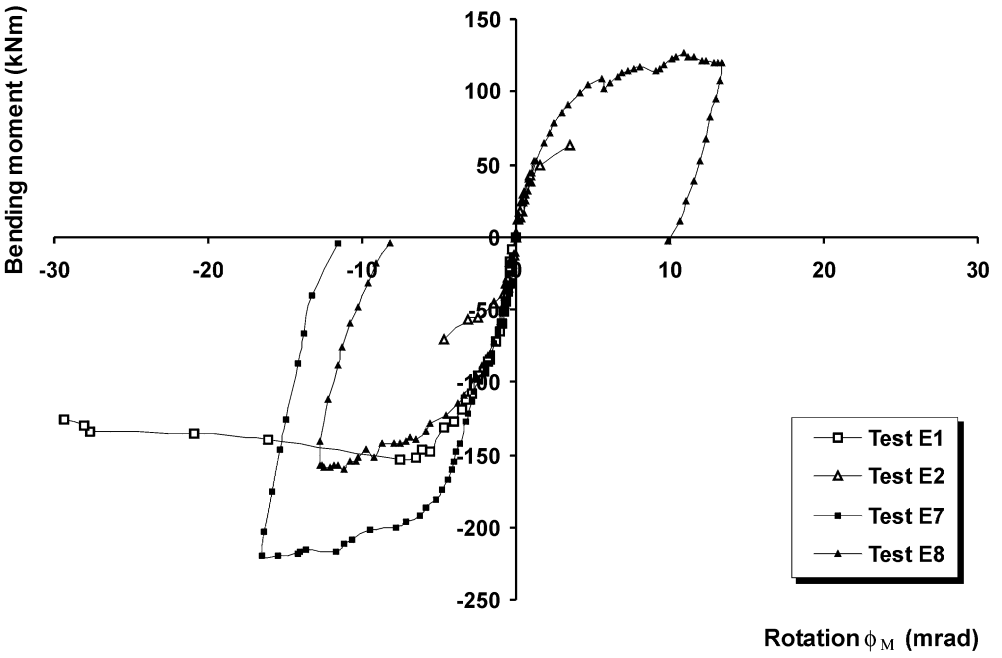

Fig. 14. Moment–rotation curves due to the deformation of the connection components.

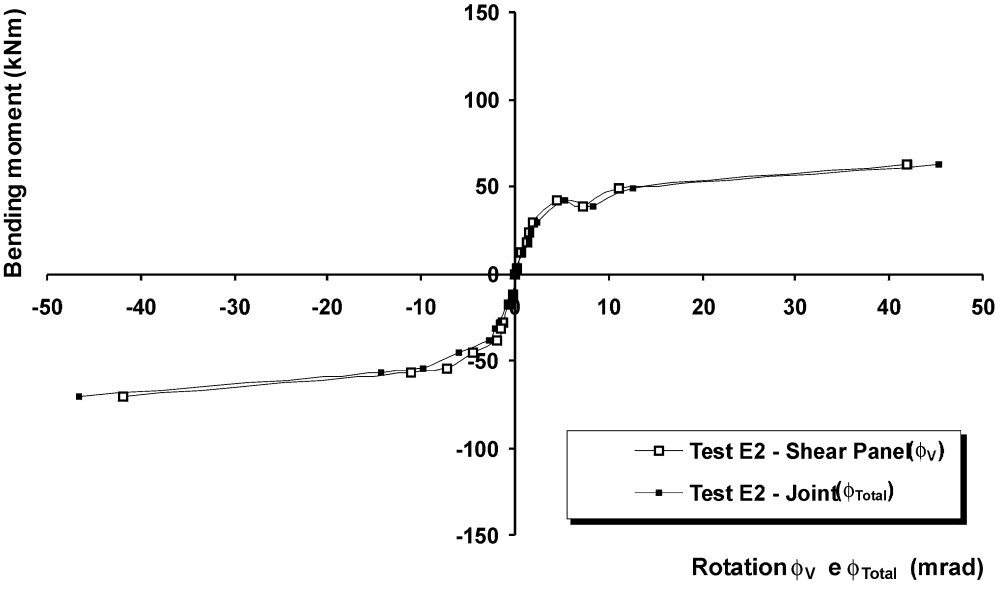

Fig. 15. Total moment–rotation curves and moment–rotation curves due to the horizontal shear deformation of the panel zone in test E2.

moments, the most current situation under gravity loading, the moment resistance may be evaluated according to the force distribution, shown in Fig. 34, where superscripts e and d refer to the left and right joints, respectively, and the various forces are defined as follows:

F_{tr} — Tensile force at the reinforcing steel.
$F_{b1}, \ldots, F_{bi}$ — Tensile forces at bolt row *i*.
F_c — Compressive force at the lower flange of the beam.
F_{cbw} — Compressive force in the beam web.
F_{cp} — Compressive force at the contact surface between the column web and the concrete slab.

Having established the various forces (components resistance according to EC3 and EC4, taking into account the influence of the other joint, in the case of internal nodes), and assuming that the neutral axis lies

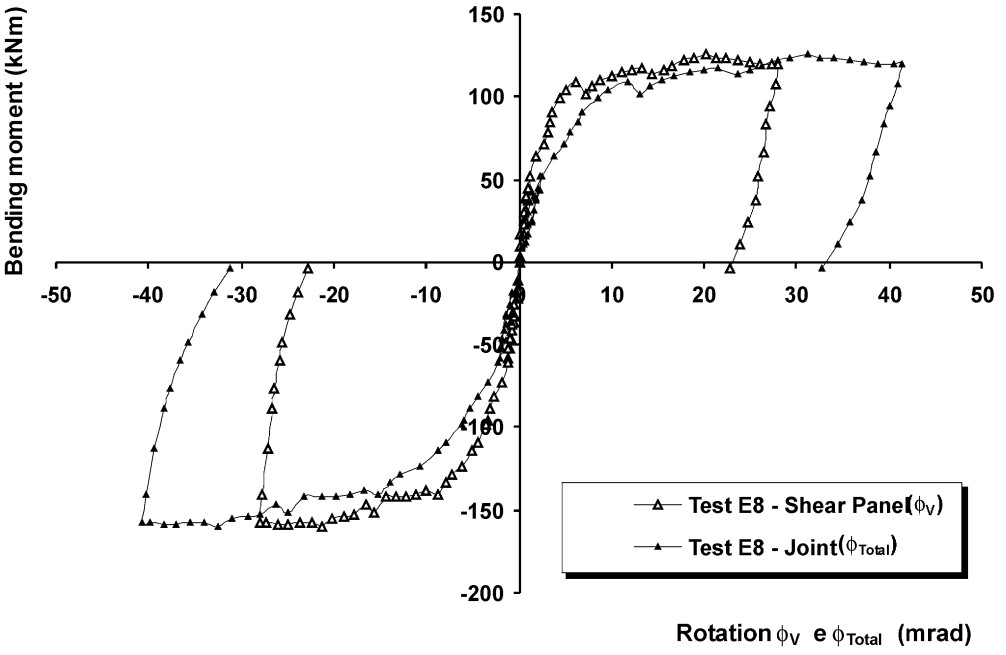

Fig. 16. Total moment–rotation curves and moment–rotation curves due to the horizontal shear deformation of the panel zone in test E8.

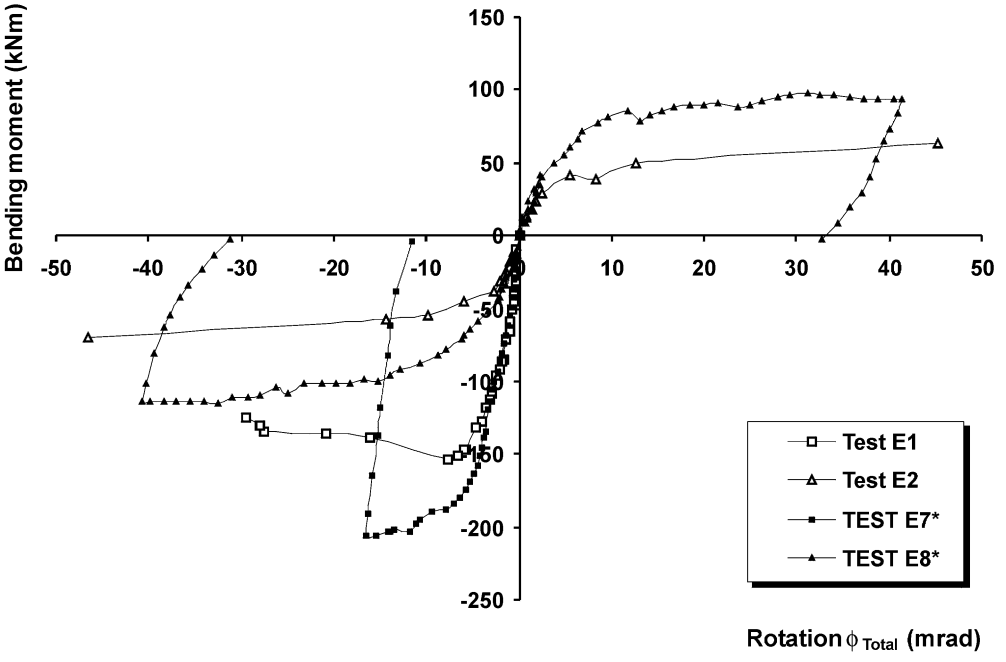

Fig. 17. Total moment–rotation curves of the joints E1, E2, E7* and E8*.

in the web of the beam (most common situation), the moment resistance ($M_{j,Rd}$) of the joint is obtained by taking moments with respect to the mid point of the beam bottom flange, yielding,

$$M_{j,Rd}=F_{tr}\cdot L_r+\sum_{i=0}^{m}(F_{bi}\cdot L_i)-h_w\cdot t_{wb}\cdot f_{ywb}\cdot\left(\frac{h_w}{2}+\frac{t_{fb}}{2}\right) \quad (1)$$

For internal nodes subjected to sagging moments or external nodes subjected to sagging or hogging moments, the evaluation of the moment resistance is similar.

The evaluation of the initial stiffness ($S_{j,ini}$) is obtained from the elastic stiffness of the components (K_i), the force–displacement relation for each component ($F-\Delta$) being given by

$$F_i=K_i\cdot E\cdot\Delta_i \quad (2)$$

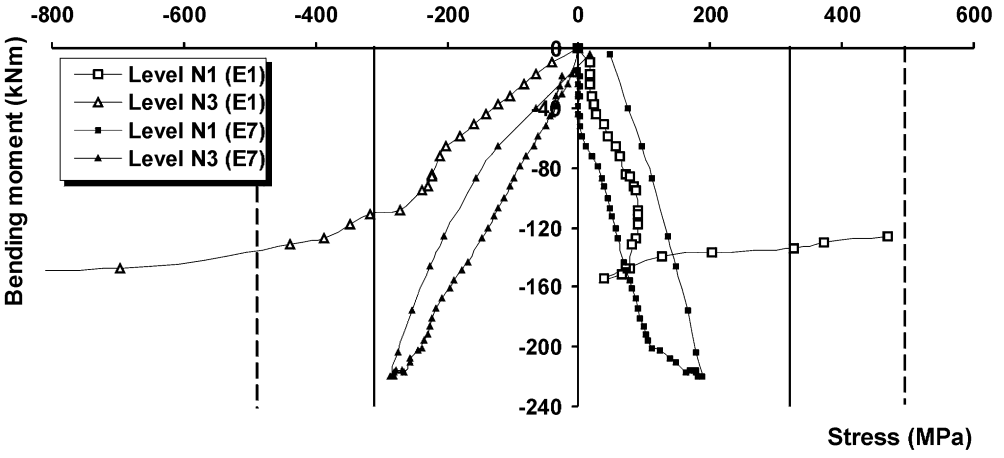

Fig. 18. Stresses in column web for tests E1 and E7.

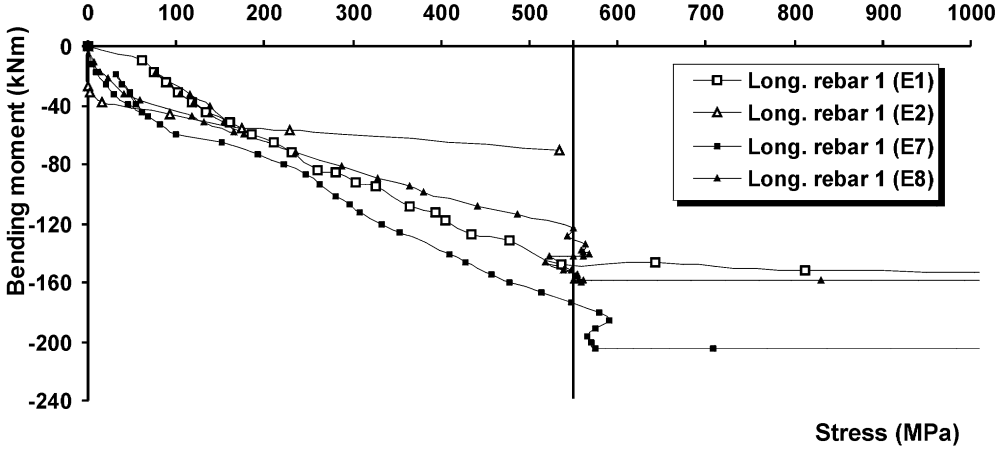

Fig. 19. Stresses in longitudinal reinforcement for internal node joints.

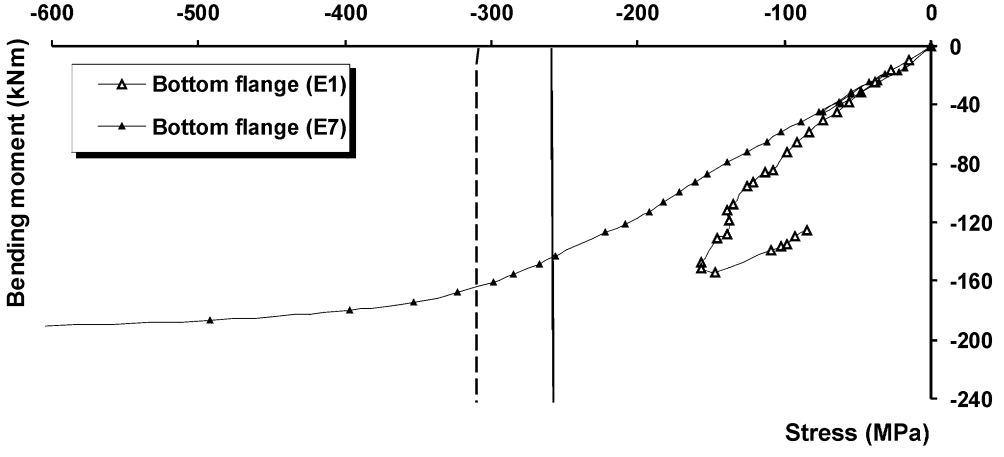

Fig. 20. Stresses in beam bottom flanges for tests E1 and E7.

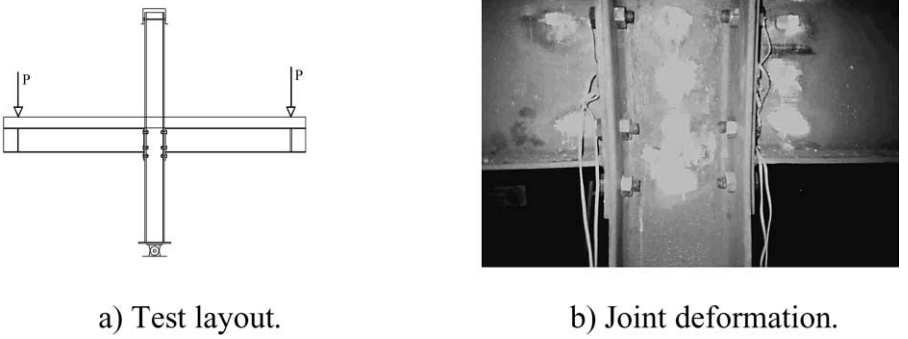

Fig. 21. Failure in test E1.

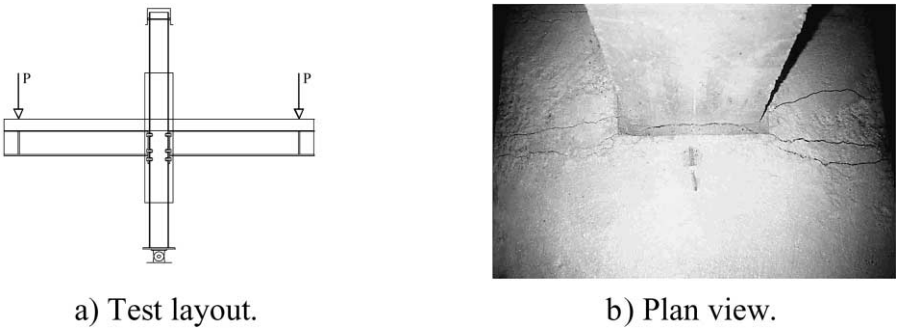

Fig. 22. Failure in test E7.

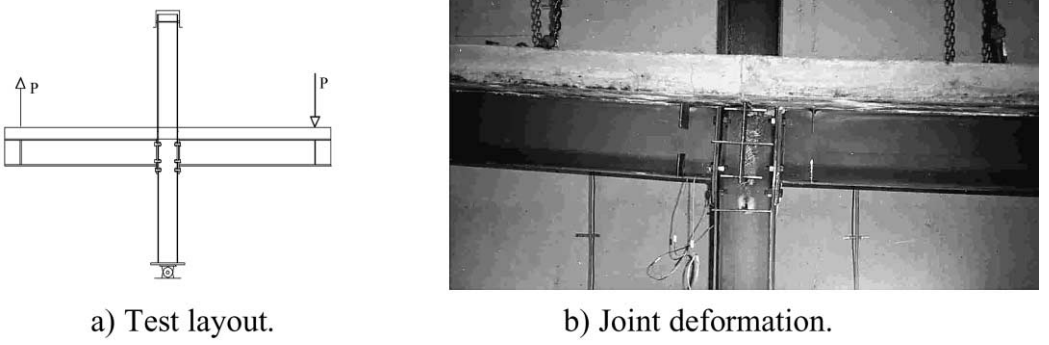

Fig. 23. Failure in test E2.

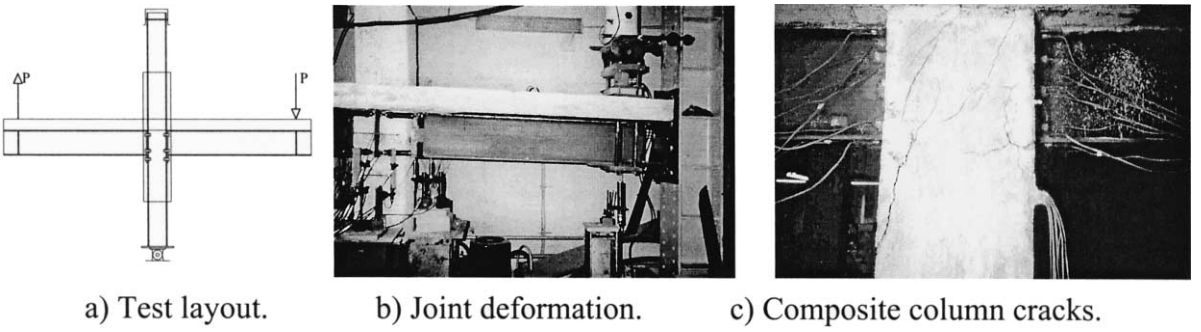

Fig. 24. Failure in test E8.

Table 8
Mechanical properties of tests E1, E2, E7 and E8

Test	Initial stiffness $S_{j,ini}$ (kNm/mrad)		Ultimate moment M_u (kNm)		Ultimate rotation ϕ_u (mrad)		Maximum rotation ϕ_{max} (mrad)		Main failure mode
	Left	Right	Left	Right	Left	Right	Left	Right	
E1		62.5		−153.6		−7.6		−29.4	Column web instability
E2	14.3	17.2	62.8	−70.5	45.3	−46.5	45.3	−46.5	Column web panel in shear
E7		81.3		−219.8		−16.5		−16.5	Slab reinforcement in tension, beam bottom flange in compression
E8	22.2	27.2	126.1	−160.2	31.2	−32.4	41.3	−40.7	Column web panel in shear

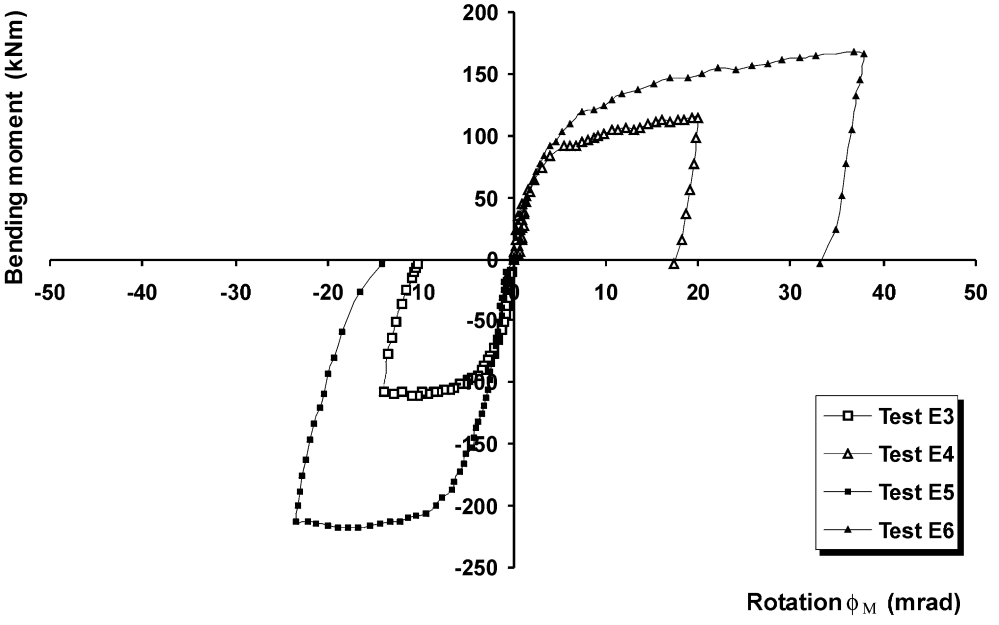

Fig. 25. Moment–rotation curves due to the deformation of the connection components.

where F_i=force developed in the component (spring) i; K_i=stiffness coefficient of the component (spring) i; E=Young's modulus of steel; Δ_i=deformation of the component (spring) i.

With reference to the spring model of a joint shown in Fig. 35, the initial stiffness is given by the following equation [30,40]:

$$S_{j,ini}=\frac{M}{\phi}=\frac{E\cdot z^2}{\sum_i \frac{1}{K_i}} \tag{3}$$

where z=lever arm; K_i=stiffness coefficient of the component i; and E is the Young's modulus of steel.

In the previous equation K_i can be replaced by $K_{eff,r}$ (association of components in series) whenever there are several components at the same level r or even by K_{eq} (association of components in parallel) if there are components with the same internal force type (tension, compression or shear) at different levels. Under these conditions, the position of the forces must be redefined (z_{eq}). According to Annex J of the EC3, $K_{eff,r}$, K_{eq} and z_{eq} are given by:

$$K_{eff,r}=\frac{1}{\sum_i \frac{1}{K_{i,r}}},\quad K_{eq}=\frac{\sum_r K_{eff,r}\cdot h_r}{z_{eq}},\quad z_{eq}=\frac{\sum_r K_{eff,r}\cdot h_r^2}{\sum_r K_{eff,r}\cdot h_r} \tag{4}$$

Given the current state-of-the-art in steel and composite joints, comparisons are restricted to strength and initial stiffness, despite some recent encoraging attempts at the analytical evaluation of the full moment–rotation response of composite joints [41,42].

Next, the experimental results are compared with the analytical predictions. It is noted that apart from the specific aspects related to the anchorage of the longitudinal reinforcement (good anchorage of the longitudinal reinforcement must be guaranteed in order to take advantage of the composite action), external node joints may be considered a particular case of internal node joints without loads on one side. Also, within the scope of the

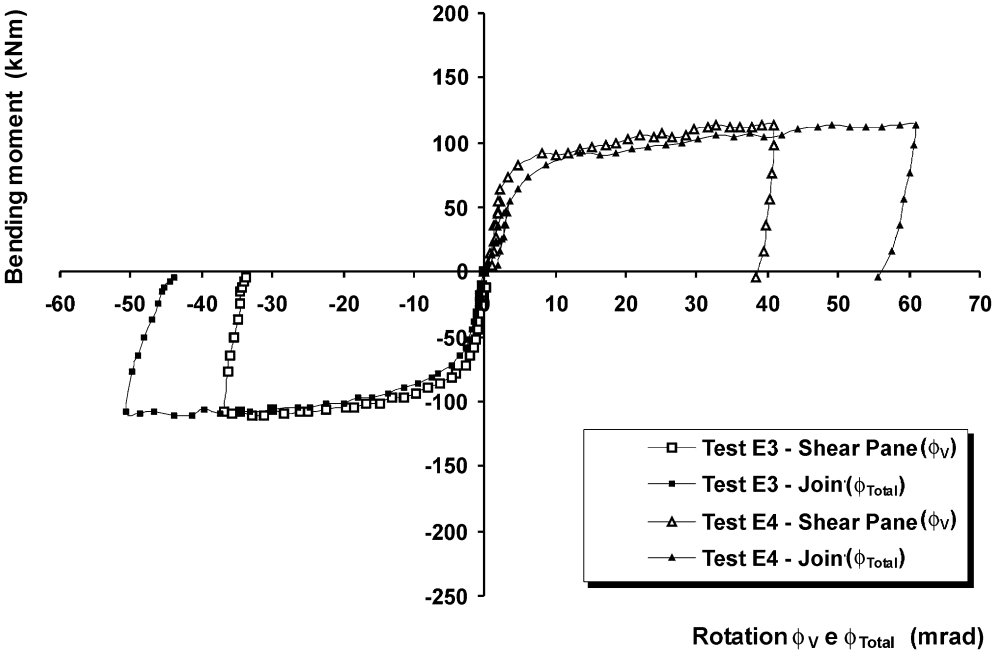

Fig. 26. Total moment–rotation curves and moment–rotation curves due to the horizontal shear deformation of the panel zone in test E2.

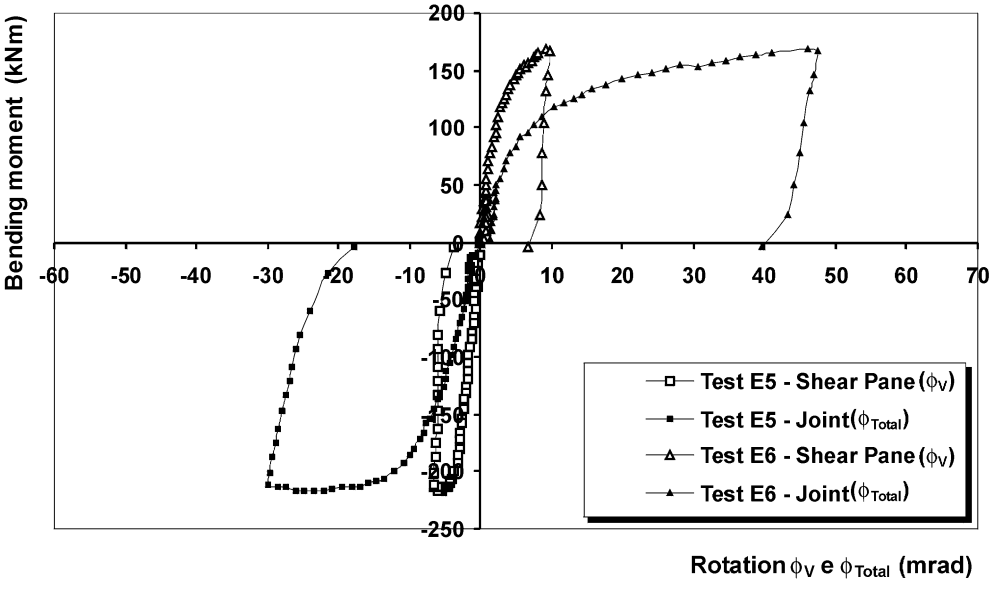

Fig. 27. Total moment–rotation curves and moment–rotation curves due to the horizontal shear deformation of the panel zone in test E8.

component method, the possibility of embedding the column with reinforced concrete (composite column) is also considered.

Actual (measured) material properties (obtained from laboratory tests and summarised in Tables 4 and 5) and measured dimensions (Tables 6 and 7) were used in the evaluation of strength and initial stiffness of the joints. Also, partial safety coefficients used in design and specified in Eurocodes 3 and 4 were taken as unity. The resulting joint moment resistance of the various joints, ($M_{j,Rd}$), is shown in Table 10. The same table compares those results with the maximum moments obtained experimentally.

Table 11 reproduces the initial stiffness of the various joints, obtained in accordance with the stiffness models of Eurocodes 3 and 4 by assembling the individual axial stiffness results for the various components. As for resistance, these values are compared with the corresponding experimental stiffness, for the various test results.

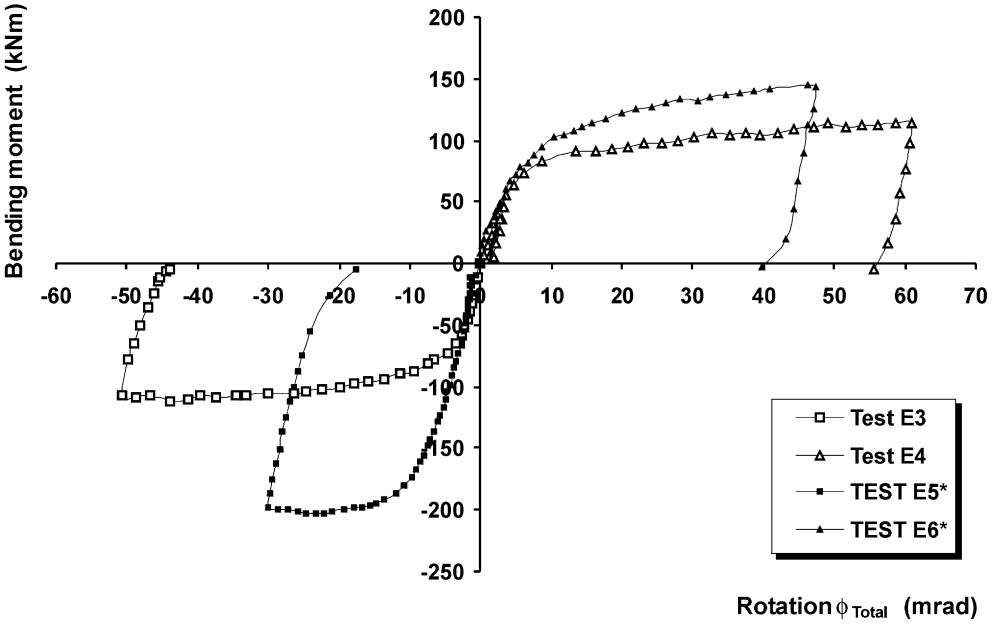

Fig. 28. Total moment–rotation curves of the joints E3, E4, E5* and E6*.

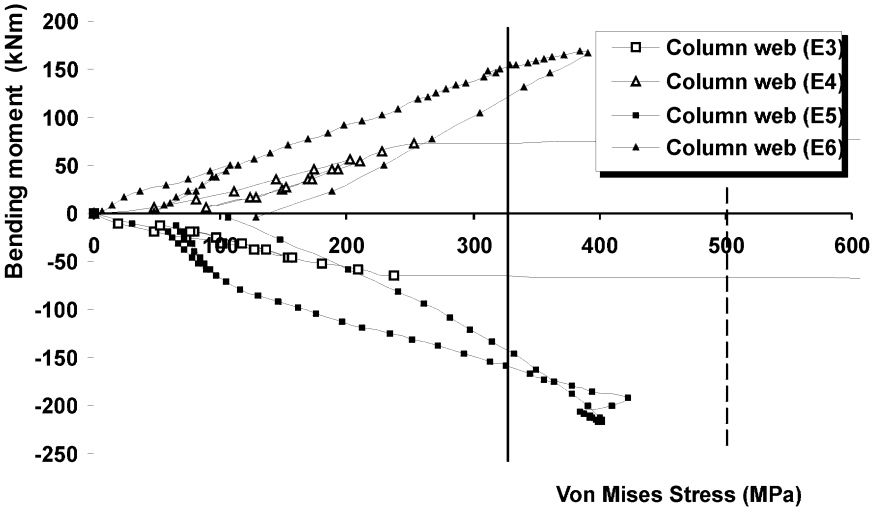

Fig. 29. Equivalent stresses (Von Mises) in column web for external node joints.

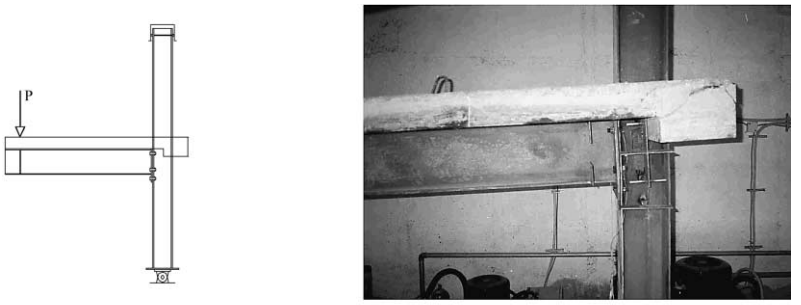

Fig. 30. Failure in test E3.

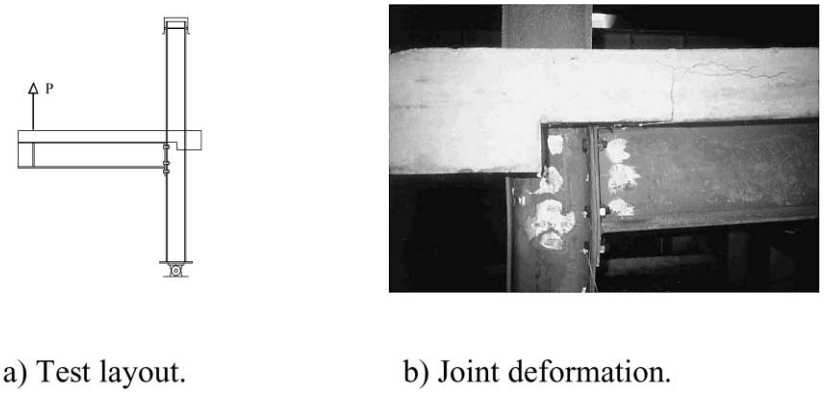

a) Test layout. b) Joint deformation.

Fig. 31. Failure in test E4.

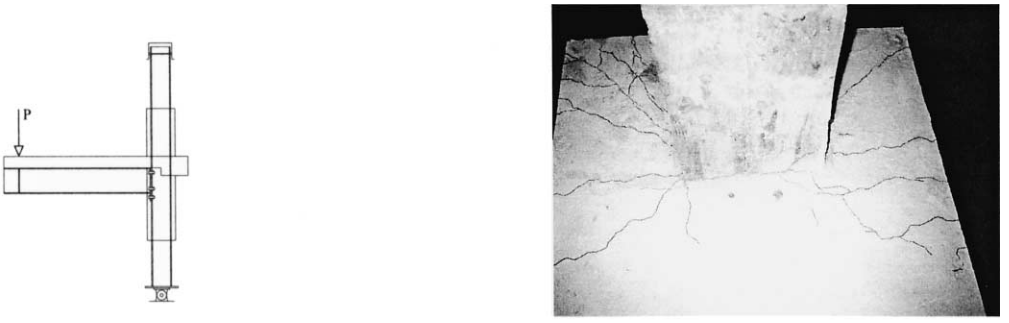

a) Test layout. b) Slab cracks.

Fig. 32. Failure in test E5.

a) Test layout. b) Joint deformation.

Fig. 33. Failure in test E6.

Figures 36 to 39 illustrate the analytical and experimental moment–rotation curves for tests E1 to E8. The analytical results are represented using a bi-linear idealisation. Table 10 and Figs 36 to 39 show that the analytical methodology developed in [36] yields safe estimates for most of the joints that were tested ($M_{j,Rd}^{anal}/M_{j,Rd}^{exp} \leq 1.0$); however, in some situations, the moment resistance obtained analytically exceeded the experimental result (maximum difference of +13%, for test E4).

In terms of initial stiffness, good agreement was achieved, always on the safe side for joints in hogging bending ($S_{j,ini}^{anal}/S_{j,ini}^{exp} \leq 1.0$); the maximum difference was −18% for test E5. For joints under sagging moment, analytical results always exceeded the corresponding experimental results, test E2 exhibiting the maximum difference of about +58%. This difference arises because current methodology neglects the deformation of the compressed concrete at the interface slab–column (crushing of concrete was in fact observed in some cases).

Table 9
Mechanical properties of tests E3, E4, E5 and E6

Test	Initial stiffness $S_{j,ini}$ (kNm/mrad)		Ultimate moment M_u (kNm)		Ultimate rotation ϕ_u (mrad)		Maximum rotation ϕ_{max} (mrad)		Main failure mode
	Left	Right	Left	Right	Left	Right	Left	Right	
E3	27.0		−111.3		−43.9		−50.8		Column web panel in shear
E4	28.7		113.2		49.0		61.0		Column web panel in shear
E5	43.1		−217.6		−22.2		−30.0		Slab reinforcement in tension, beam bottom flange and web in compression
E6	44.4		168.2		46.2		47.5		End plate and column flange in bending

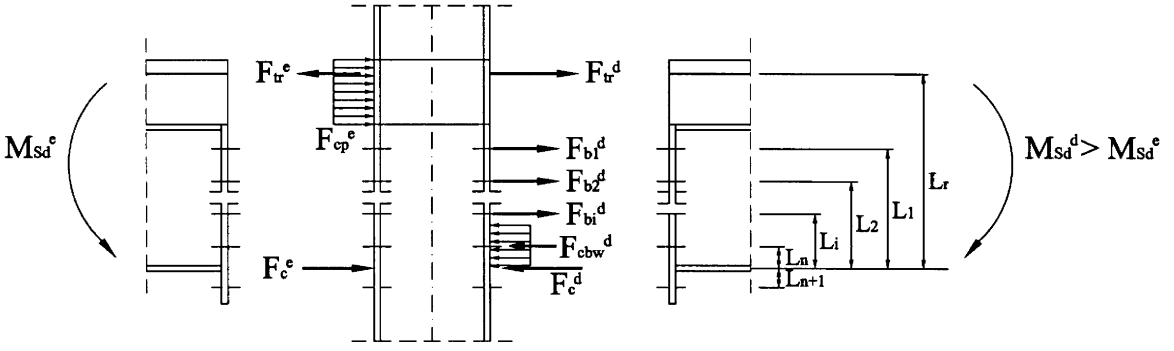

Fig. 34. Distribution of forces in an internal node subjected to unequal hogging moments.

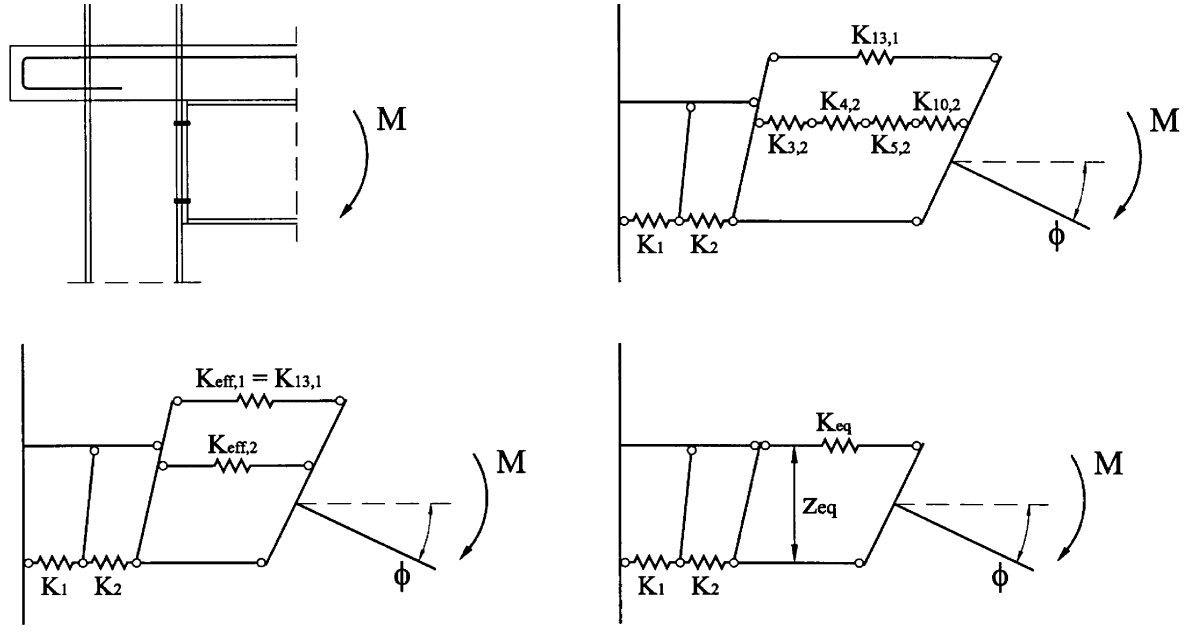

Fig. 35. Spring model of a composite joint.

6. Conclusions

The experimental research program described in this paper led to the following conclusions:

- Joints between composite beams and steel columns under static monotonic loading (tests E1 to E4) exhibited high ductility;
- Joints between composite beams and steel columns

Table 10
Moment resistance: experimental ($M_{j,Rd}^{exp}$) and analytical ($M_{j,Rd}^{anal}$)

Test	$M_{j,Rd}^{exp}$ (kNm)		$M_{j,Rd}^{anal}$ (kNm)		$M_{j,Rd}^{anal}/M_{j,Rd}^{exp}$	
	Positive	Negative	Positive	Negative	Positive	Negative
E1		−153.60		−140.78		0.92
E2	62.80	−70.50	65.53	−72.96	1.04	1.03
E7		−219.80		−220.84		1.00
E8	126.10	−160.20	124.51	−168.03	0.99	1.05
E3		−111.30		−108.56		0.98
E4	113.20		128.03		1.13	
E5		−217.60		−218.82		1.01
E6	168.20		155.06		0.92	

Table 11
Initial stiffness: experimental ($S_{j,ini}^{exp}$) and analytical ($S_{j,ini}^{anal}$)

Test	$S_{j,ini}^{exp}$ (kNm/mrad)		$S_{j,ini}^{anal}$ (kNm/mrad)		$S_{j,ini}^{anal}/S_{j,ini}^{exp}$	
	Positive	Negative	Positive	Negative	Positive	Negative
E1		62.50		57.76		0.92
E2	14.30	17.2	22.55	16.85	1.58	0.98
E7		81.30		76.69		0.94
E8	22.20	27.20	33.00	24.70	1.49	0.91
E3		27.00		25.31		0.94
E4	28.70		38.38		1.34	
E5		43.10		35.41		0.82
E6	44.40		51.83		1.17	

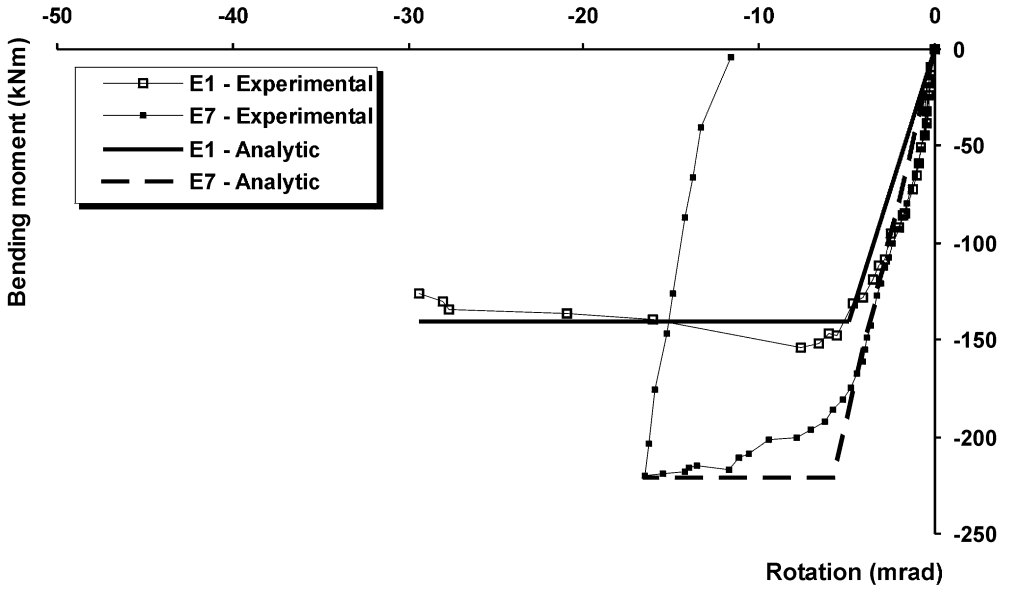

Fig. 36. Moment–rotation curves for tests on internal nodes under symmetrical loading (E1 and E7).

under symmetrical loading, such as test E1, have shown high strength and initial stiffness. On the other hand, tests with asymmetrical loading (test E2 and external node tests E3 and E4), were mostly governed by the column web panel deformation in shear, leading to reduced values of strength and initial stiffness;

- Joints where both column and beam are composite (E5 to E8), tested under similar load conditions to tests E1 to E4, resulted in an increase of strength and initial stiffness without significant reduction of ductility, because of the stiffening effect of concrete on the column web panel.

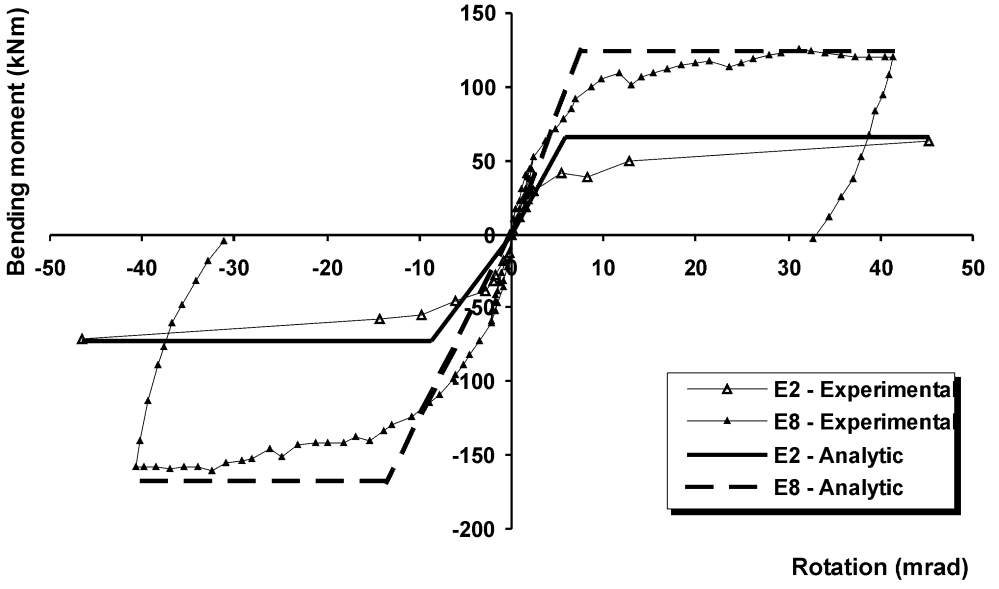

Fig. 37. Moment–rotation curves for tests on internal nodes under anti-symmetrical loading (E2 and E8).

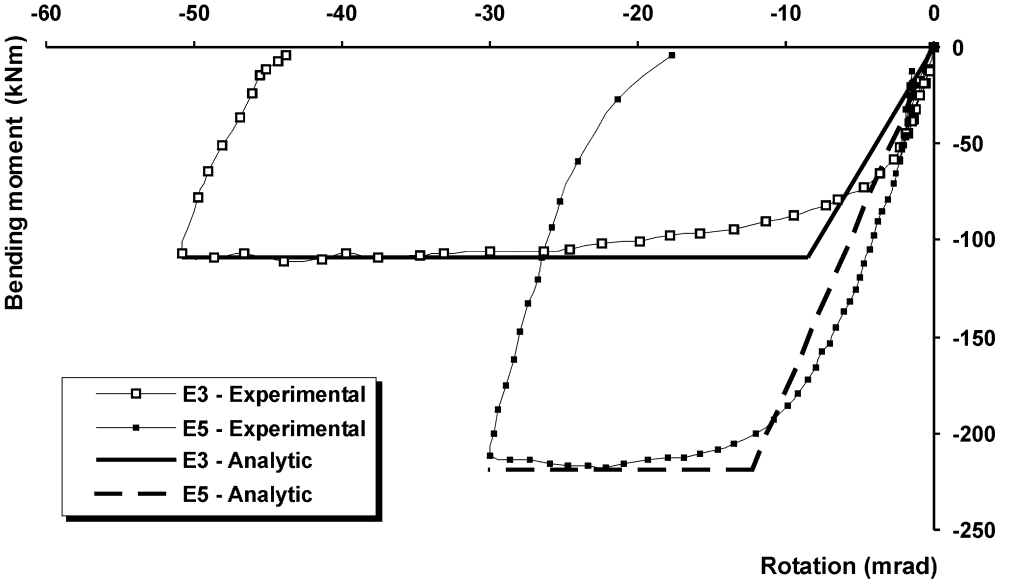

Fig. 38. Moment–rotation curves for tests on external nodes under negative moment (E3 and E5).

Additionally, based on the methodology developed for the analytical evaluation of composite joints [36], the following conclusions may be established:

- The analytical methodology accurately reproduces strength and initial stiffness for most of the tested configurations;
- Even for joints under sagging bending (left joints in tests E2 and E8 and joints E4 and E6), a situation not yet covered by Section 8 of Eurocode 4, good agreement was noted in terms of moment resistance;
- In contrast, initial stiffness for this latter case was over-estimated. This discrepancy resulted from neglecting the deformation of the compressed concrete at the interface column–slab (a component still requiring a considerable research effort).

Acknowledgements

Financial support from Ministério da Ciência e Tecnologia — PRAXIS XXI research project

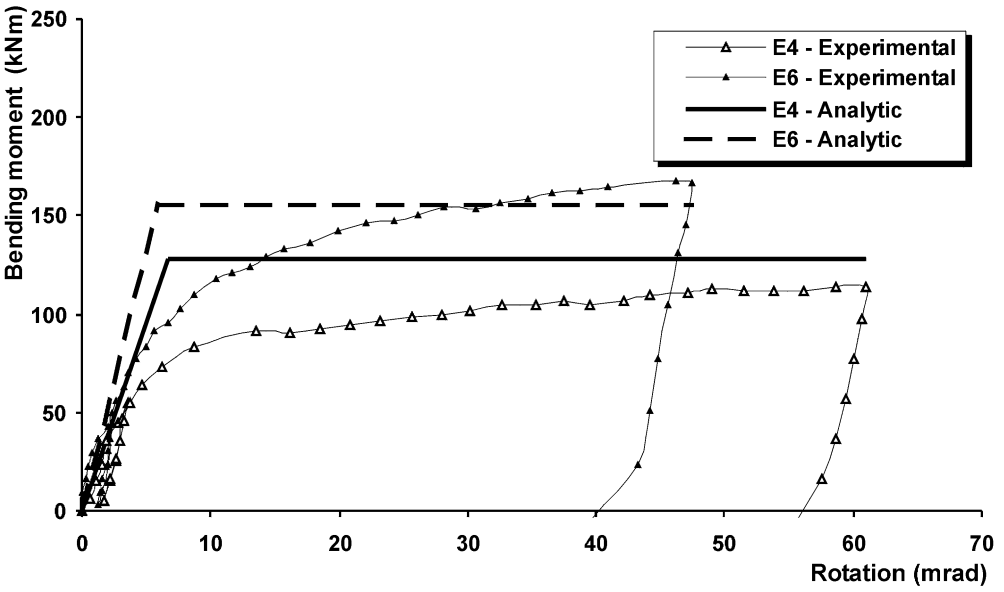

Fig. 39. Moment–rotation curves for tests on external nodes under positive moment (E4 and E6).

PRAXIS/P/ECM/13153/1998 and PRODEP II (Sub-programa 1) is acknowledged.

References

[1] Anderson D, editor. COST C1 Composite steel–concrete joints in braced frames for buildings. Brussels–Luxembourg, 1996

[2] CEN, Eurocode 4 — Design of composite steel and concrete structures — Part 1.1 (Draft no. 1): General rules and rules for buildings, prEN 1994-1-1: 2001.

[3] CEN, Eurocode 3 — Design of steel structures — Part 1.1: General rules and rules for buildings, ENV 1993-1-1, 1998.

[4] Zandonini R. Semi-rigid composite joints. In: Narayanan R, editor. Structural Connections: Stability and Strength. London: Elsevier Applied Science, 1989:63–120.

[5] Ahmed B, Nethercot DA. Prediction of initial stiffness and available rotation capacity of major axis composite flush endplate connections. Journal of Constructional Steel Research 1997;41(1):31–60.

[6] Couchman G, Way A, editors. Joints in Steel Construction — Composite Connections, SCI-P-213.: SCI, 1998.

[7] Davison JB, Lam D, Nethercot DA. Semi-rigid action of composite joints. Structural Engineer 1990;68(24):489–99.

[8] Leon RT. Semi-rigid composite construction. Journal of Constructional Steel Research 1990;15:99–120.

[9] Puhali R, Smotlak I, Zandonini R. Semi-rigid composite action: experimental analysis and a suitable model. Journal of Constructional Steel Research 1990;15(1–2):121–51.

[10] Altmann R, Maquoi R, Jaspart JP. Experimental study of the nonlinear behaviour of beam-to-column composite joints. Journal of Constructional Steel Research 1991;18(1):45–54.

[11] Aribert JM, Lachal A. Experimental investigation of composite connections and global interpretation. In: Colson A, editor. COST C1 — Semi-rigid behaviour of civil engineering structural connections. Strasbourg, 1992:158-169.

[12] Xiao Y, Choo BS, Nethercot DA. Composite connections in steel and concrete — I. Experimental behaviour of composite beam–column connections. Journal of Constructional Steel Research 1994;31(1):3–30.

[13] Anderson D, Najafi AA. Performance of composite connections: major axis end plate joints. Journal of Constructional Steel Research 1994;31(1):31–57.

[14] Sedlacek G, Weynand K, Byung-Seung Kong, Saal H, Klinkenberg A, Bode H, Kronenberger H. Research work done in Germany in the field of semi-rigid connections. In: Wald F, editor. COST C1 — Semi-rigid behaviour of civil engineering structural connections. Prague, 1994:121-130.

[15] Li TQ, Nethercot DA, Choo BS. Behaviour of flush end-plate composite connections with unbalanced moment and variable shear/moment ratios — I. Experimental behaviour. Journal of Constructional Steel Research 1996;38(2):125–64.

[16] Benussi F, Bernuzzi C, Noe S, Zandonini R. Experimental analysis of semi-rigid composite frames. In: Proceedings of IABSE Colloquium — Semi-rigid structural connections, Istanbul, 1996:105–14.

[17] Benussi F, Nethercot DA, Zandonini R. Experimental behaviour of semi-rigid connections in frames. In: Bjorhovde R, Colson A, Zandonini R, editors. Proceedings of the Third International Workshop — Connections in Steel Structures III — Behaviour, Strength and Design, Trento University, 29-31 May. Oxford: Pergamon, 1995:57–66.

[18] Li TQ, Moore DB, Nethercot DA, Choo BS. The experimental behaviour of a full-scale, semi-rigidly connected composite frame: Overall considerations. Journal of Constructional Steel Research 1996;39(3):167–91.

[19] Li TQ, Moore DB, Nethercot DA, Choo BS. The experimental behaviour of a full-scale, semi-rigidly connected composite frame: Detailed appraisal. Journal of Constructional Steel Research 1996;39(3):193–220.

[20] Choo B, Li T, Nethercot DA, Xiao Y. Behaviour and design of composite connections. In: Colson A, editor. COST C1 — Semi-rigid behaviour of civil engineering structural connections. Strasbourg, 1992:170-181.

[21] Bernuzzi C, Noe S, Zandonini R. Semi-rigid joints: Experimental studies. In: Bjorhovde R, Colson A, Haaijer G, Stark G, Stark JWB editors. Connections in steel structures II: Behaviour, strength, and design. Pennsylvania, 1991:189-200.

[22] Tschemmernegg F. Non-linear behavior of composite joints. Journal of Constructional Steel Research 1992;21(1–3):59–70.

[23] Badran M. Tests on semi-rigid composite joints. In: Wald F, editor. COST C1 — Semi-rigid behaviour of civil engineering structural connections. Prague, 1994:141-146.
[24] Ren P. Numerical modelling and experimental analysis of steel beam-to-column connections allowing for the influence of reinforced-concrete slabs. Ph.D. Thesis, Lausanne, 1995.
[25] Shanmugam NE, Yu CH, Richard JY, Teo TH. Modelling of steel–concrete composite joints. Journal of Constructional Steel Research 1998;46(1–3):000–0 paper 138.
[26] Wong YL, Wang JY, Chan SL. Effects of loading conditions on behaviour of semi-rigid beam-to-column composite connections. In:, 1999:451–8.
[27] Elnashai AS, Broderick BM, Dowling PJ. Earthquake-resistant composite steel/concrete structures. Structural Engineer 1995;73(8):121–32.
[28] Jaspart JP, Maquoi R. Investigation by testing of the structural response of semi-rigid joints. In: Mazzolani FM, editor. Testing of Metals for Structures. London: E. and F.N. Spon, 1992:53–63.
[29] Lourenço J, Coutinho J. O cálculo automático no projecto de composição de betões. Série Monografias Técnicas, Coimbra, 1986.
[30] CEN, Annex J for Eurocode 3 — Joints in building frames. ENV 1993-1-1:1992/A2, October 1998.
[31] EN 10002 — Metallic materials: Tensile testing, 1990/2.
[32] EN 10020 — Steel definition and classification, 1989.
[33] EN 10025 — Hot rolled products of non-alloy structural steels, 1994.
[34] ENV 206 — Concrete: performance, production, placing and compliance criteria, 1993.
[35] CEN, Eurocode 2 — Design of concrete structures — Part 1: General rules and rules for buildings, ENV 1992-1-1:1991.
[36] Simões R. Behaviour of beam-to-column composite joints under static and cyclic loading [in Portuguese]. Ph.D. Thesis, Civil Engineering Department, University of Coimbra, Coimbra, 2000.
[37] SCI, Moment connections in composite construction: Interim guidance for end-plate connections, Prepared by R. M. Lawsen and C. Gibbons, SCI-P-143, 1995.
[38] Jaspart JP, editor. COST C1 — Recent advances in the field of structural steel joints and their representation in the building frame analysis and design process, Brussels–Luxembourg, 1999.
[39] Li TQ, Nethercot DA, Choo BS. Behaviour of flush end-plate composite connections with unbalanced moment and variable shear/moment ratios — II. Prediction of moment capacity. Journal of Constructional Steel Research 1996;38(2):165–98.
[40] ECCS. Design of composite joints for buildings, Prepared by Technical Committee 11 — Composite Structures, Publication 109, 1999.
[41] Simões Da Silva L, Girão A, Simões R. Analytical Evaluation of the Moment-Rotation Response of Composite Joints under Static Loading. International Journal of Steel and Composite Structures 2001;1(2):245–68.
[42] Huber G. Nicht-lineare berechnungen von verbundquerschnitten und biegeweichen knoten. Ph.D. Thesis [in English], University of Innsbruck, Austria, 1999.